Two-component superconductivity. I. Introduction and phenomenology

Y. Bar-Yam
Materials Research Department, Weizmann Institute of Science, Rehovot 76100, Israel
(Received 11 July 1990)

A two-component theory of superconductivity is developed where one electronic component provides mobility and the other provides pairing. For the Cu-O-based high-T_c materials the two components are identified with mobile electronic states associated with Cu-O planes, and localized negative-U states associated with oxygen vacancies in the Cu-O planes. An explicit comparison of phenomenology with BCS theory is performed including comparison with experiments on $YBa_2Cu_3O_7$. The discussion includes quantitative comparison of the superconducting properties T_c, Δ, H_c, and ξ. Long-wave collective excitations, normal-state properties including resistance and tunneling, and the isotope shift are described. Unusual properties are predicted including neutral-fermion excitations, a spreading of the fermionic gap onset, a separation between the resistive transition T_c' and the evaporation of the condensate T_c, anomalies in sound and bulk modulii at T_c, linear temperature dependence of normal-state resistivity, linear voltage dependence in normal-state tunneling conductance, and finite zero-bias conductance in superconducting-state tunneling. A new signature of structural coherence obtained by channeling experiments is indicated.

There are two attributes of electrons for superconductivity: mobility and pairing. While this is not directly obvious, these two attributes compete against each other.[1,2] Large pairing energies are consistent with poor mobility and high mobilities are consistent with weak pairing. In this article a theory of superconductivity is described based on combining these two attributes by making use of two types of electronic states in the same material, one which provides mobility and the other pairing. A small hybridization between the two types of states is essential for the mobility and pairing to work together to give superconductivity. Further, it is suggested that many diverse experiments on high-T_c materials can be understood within such a theory where (1) locally paired states are associated with *oxygen vacancies* in Cu-O planes and (2) mobile single-particle states, are associated with *Cu-O planes*. Superconductivity arises because the localized states become mobile through partial mixing with the extended states, and the extended states become paired through mixing with the locally paired states.

Localized pairing is the local analog of Cooper pairing of extended states—it is accomplished through the electron-ion (electron-phonon or electron-structural relaxation) interaction. Localized states which pair are known as negative-U centers,[3] where U is the effective electron-electron repulsion.

The oxygen vacancies responsible for the paired states are located in the Cu-O planes. Because of this, the introduction of localized states by oxygen vacancies also disrupts the mobile states. In large part, it is the combination of constructive and destructive roles of the oxygen vacancies which has led to difficulties in the interpretation of experimental literature. Basic theoretical phenomenology is discussed here while a discussion of the family of high-T_c materials is pursued in a companion article.

There are two objectives to this article, (1) to introduce a conceptual understanding of the theory and (2) to discuss the phenomenology providing predictions which can motivate experimental tests. The understanding of the theory described here is still preliminary. A key point of this discussion is the comparison of the two-component theory with Bardeen, Cooper, and Shrieffer's (BCS) theory of superconductivity in metals.[4,5] Surprisingly, many basic differences exist. Comparisons are also made with the theory of strong-pairing low-mobility superconductivity known as negative-U lattice theory. Discussions of antiferromagnetism (which can be accounted for by a repulsive interaction of single-particle states[6]), low-dimensional structural components in Cu-O-based materials, and disorder, which play a major role in phenomenology and other theoretical approaches to superconductivity,[7,8] are largely postponed since they do not play an essential role in the superconductive properties to be derived.

This article is divided into three sections. In the first, the theoretical background is briefly summarized. The second introduces pictorially the two-component theory and then an appropriate formalism. The third section describes the general phenomenology of the two-component theory with application to $YBa_2Cu_3O_7$. Included in this discussion are the following: (a) The transition temperature and the fermionic gap T_c, and Δ; (b) the thermodynamic critical field H_c; (c) the coherence length ξ; (d) long-wavelength collective excitations; (e) normal-state properties; and (f) the isotope shift and a new signature of structural coherence.

I. THEORETICAL BACKGROUND

BCS theory describes the superconductivity arising from a weak pairing interaction of mobile extended electrons.[4] When the pairing is stronger but the electrons can still be described as extended, strong-coupling theory applies.[9] For an even stronger interaction, or for inherently localized paired electrons (negative-U lattice) it

has been suggested that a superconductivity arises in the form of a Bose condensation of preexisting tightly bound pairs similar to liquid-He^4 condensation.[10–12] No physical realization of this is known. In this limit the mobility is low because of the strong electron attraction, the inherent localization of the electrons, and the strong coupling to the lattice relaxation responsible for the pairing. It is this mobility which controls the transition temperature T_c. Since no physical realization is known, it is not clear that such states by themselves can be mobile. Strong localized pairing is well established in localized states associated with defects in semiconductors where it has been discussed[13,14] and studied theoretically[15–18] and experimentally.[19,20] The enhancement of superconductivity in metal-semiconductor disordered alloys[21,22] motivated studies of negative-U localized pairing states in a metal and their enhancement of BCS superconductivity of the metal.[23–25] The idea of superconductivity induced by resonant pairs[26] predates BCS theory, was reintroduced,[27,28] and has been suggested as relevant for the high-T_c materials[29–33] with pairing possibly arising from electron many-body effects. General arguments suggesting local pairing in the high-T_c materials have been given.[34,35] Treatment of two types of *mobile* electrons in a metal and the hybridization contribution to superconductivity is known as two-band superconductivity.[36–39] The key suggestion that oxygen vacancies in high-T_c materials can be responsible for enhanced pairing has been discussed.[40,41] The single-particle electronic stats associated with oxygen vacancies have been calculated yielding localized states with transition energies near the Fermi energy.[42,43] Each of these works contains some of the basic concepts of the theory which is described here. The phenomenology which is to be described and its relationship to material properties is unique to the two-component theory developed here.

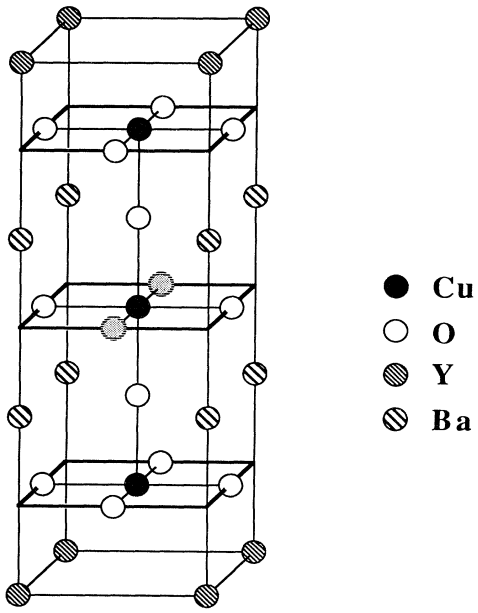

FIG. 1. Diagram of one unit cell of the structure of $YBa_2Cu_3O_7$ (1:2:3:7 material). The structure is layered, formed out of alternating Cu-O planes [Fig. 2(a)] and ionic (insulating or semiconducting) layers. The central one of the three Cu-O planes is incomplete, half of the oxygen atoms are missing (shaded circles), forming Cu-O chains [Fig. 2(b)]. Mobile electronic states are associated with the Cu-O planes and chains. An ordered lattice of localized states is naturally associated with the missing oxygen atoms since the same type of state arises when only one oxygen atom is missing in a plane [Fig. 2(c)]. The insulating layers are important in establishing the confinement of the localized states.

II. INTRODUCTION TO THE TWO-COMPONENT THEORY

A. Pictures

To motivate the basics of the theory, Fig. 1 shows an idealized picture of the extensively studied structure of $YBa_2Cu_3O_7$ (1:2:3:7 material).[44] The structure is layered with Cu-O bonded planes [Fig. 2(a)] and ionic (insulating or semiconducting) layers in between. One of three Cu-O planes is incomplete; half of the oxygen atoms are missing thus forming Cu-O chains [Fig. 2(b)]. While it may seem natural to think about the Cu-O chains, it proves natural to associate one localized electronic state per unit cell with the missing oxygen sites. Similar states arise when an oxygen atom is removed from a complete plane [Fig. 2(c)].[30,31] Thus we consider an ordered lattice of localized defect states. The Cu and O in complete planes are tightly bound and give rise to a band of mobile states which are partially occupied.

The electronic states for the two-component theory are abstracted from this picture of 1:2:3:7 material without a direct one-to-one correspondence. A schematic picture of the essential electronic states for the two-component theory is illustrated in Figs. 3 and 4. A lattice of localized states coexists with a lattice of mobile states. The central assumption of this theory is that the localized states are negative-U centers. This means that if electrons are placed in the localized states they prefer to pair so that each site is either doubly occupied or unoccupied (Fig. 5). This assumption can be checked theoretically by calculations similar to those used to study localized negative-U states in semiconductors.[15–18] Experimental manifestations are the subject of this and the companion article.

The mobile states have a large hopping (overlap) between adjacent sites which gives rise to their mobility. A small hopping is also possible between the locally paired states and the mobile states. This hopping could involve single particles, or pairs, but since leaving one particle on a paired site would have a high energy it would rapidly move into the mobile states or another mobile electron would join it, so that single-particle processes can be folded into the pair hopping processes in perturbation theory. Thus we only need to consider either full or empty paired sites for most of the theoretical discussion.

Direct hopping between the paired states may be possible and would affect some aspects of the following discussion. It will be assumed that such hopping is weak and it will be shown that the mobility of the single-particle

states can be effective in leading to mobility of the paired states. The mobile states may also have an attractive or repulsive effective electron-electron interaction. The effect of coupling to the paired band is diminished if the mobile states are inherently paired. On the other hand, a repulsive electron-electron interaction causes the up and down electrons to hop onto paired sites from different origins, and leads to competition of superconductivity with antiferromagnetism [Fig. 4(c)]. Central points of the theoretical development can be made assuming that the electron-electron interaction is weak on the mobile states.

In order to describe the elements of two-component theory, it is convenient first to consider the two types of states without coupling: allowing the paired states to possess the mobility which is to be gained by coupling to the mobile states, and the mobile states to have the pairing which is to be gained by coupling to the paired states.

Paired states. A lattice of paired states, when partially filled, is a bosonic system like liquid He^4. The boson density is changed by the Fermi energy μ of the electrons. They are charged. In the usual simple bosons, the Fermi energy must lie below the lowest bosonic state. These, however, are "hard-core" bosons, since two pairs cannot sit on the same site. At half-filling of the paired states there is pair particle-hole symmetry. Above half-filling we can talk about the pair holes as bosons and below half-filling the pairs as bosons. At $T=0$ the pair density is just a linear function of the Fermi energy. The effective boson number behaves as $n_B(1-n_B)$ where n_B is the fractional occupation of sites. The fractional filling and boson number are shown as a function of μ in Fig. 6.

In a bosonic system, boson condensation occurs below a temperature related to the mobility[45] of the bosons, the higher the mobility (or the lower the mass) the higher is the condensation temperature. Superfluidity occurs below the transition temperature. Bosonic states with a definite momentum q are generated in the usual way:

$$B_q^\dagger = \frac{1}{\sqrt{N}} \sum_i e^{-iqR_i} B_i^\dagger , \tag{1}$$

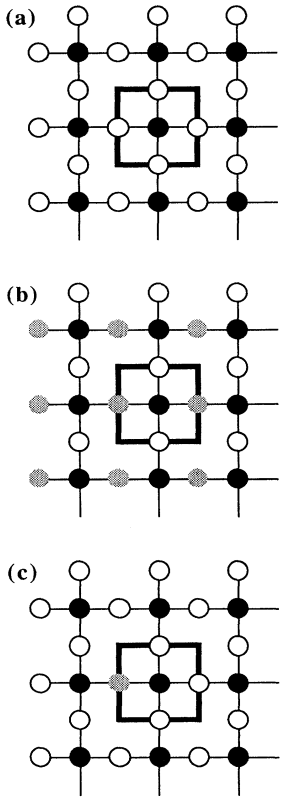

FIG. 2. (a) Complete Cu-O plane which gives rise to extended single-particle states in the two-component theory of superconductivity. The square indicates the cross section of the unit cell of Fig. 1. (b) Incomplete Cu-O plane. The shaded circles are locations of oxygen vacancies when compared with the full Cu-O plane. There are two types of electronic states expected to be associated with the incomplete plane. One is similar to the complete Cu-O plane. The other is a set of localized states identifiable with the oxygen vacancies. (c) Oxygen vacancy in the Cu-O plane. The ordered lattice of oxygen vacancies motivates the formalism of the two-component theory.

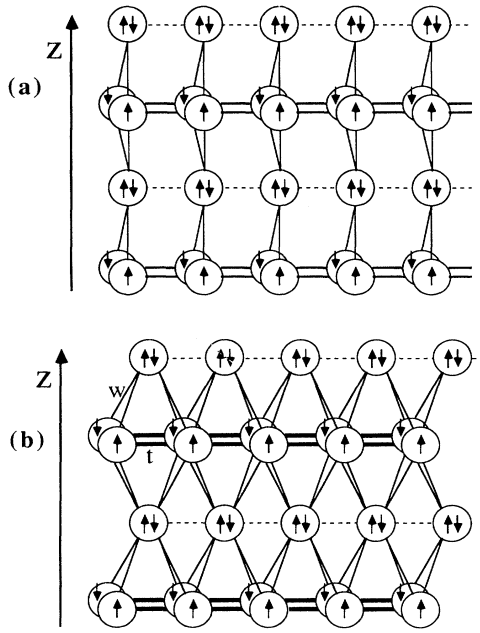

FIG. 3. Illustrations of the essential states for the two-component theory. This diagram is not meant to exactly give the electronic states of the 1:2:3:7 material but to capture the two kinds of states: (1) localized states assumed to be negative-U centers (see Fig. 5) shown by circles with paired up-down arrows, and (2) single-particle extended states, illustrated by separating spin-up from spin-down. Each horizontal set of states schematically represents a plane in 1:2:3:7 material. The localized states are associated with the oxygen vacancies in the incomplete Cu-O plane, and the single-particle states with the complete planes. One plane of single-particle states replaces the two complete Cu-O planes in 1:2:3:7 material. The hopping of the single-particle states t is large. A small hopping (w) of electrons from the paired states into the single-particle states, or vice versa, is possible. (a) shows a conceptually simple way for the planes to be connected to the paired states, while (b) shows slightly more realistic connections where the difference is of importance for the mobility of the pairs induced by hopping through the single-particle states.

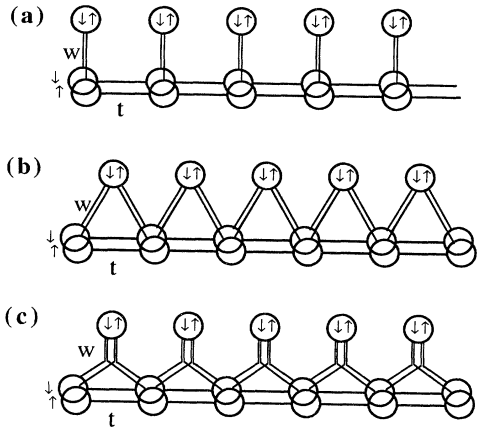

FIG. 4. The building blocks for different ways of connecting paired and single-particle states. In (a) each pair can hop only to one single-particle site. In (b) each single-particle site is shared between paired sites. The difference between (a) and (b) affects the probability of a pair hopping into the single-particle states and back onto the same site. This "self-hopping," larger in (a) than (b), is not helpful in generating superconductive correlations and is manifest in the formalism through E_q^0. In the case of a repulsive interaction in the single-particle states, two electrons hopping onto a paired site will originate at different single-particle sites as illustrated in (c). Antiferromagnetism in the Cu-O-based materials suggests that such a repulsion should be assumed and thus (c) is the most realistic coupling for these materials. While antiferromagnetic order competes with superconductivity, the existence of this type of hopping suggests that a repulsion on the single-particle states does not fundamentally interfere with superconductivity. Most of the basic concepts developed in this article are independent of the nature of the couplings (a), (b), and (c).

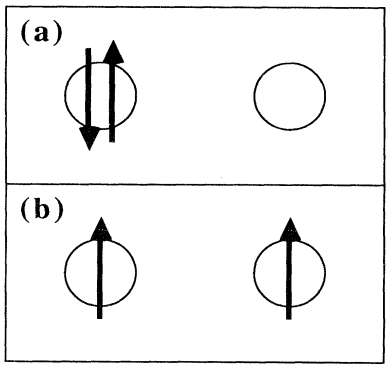

FIG. 5. A negative-U center is the localized analog of Cooper pairing of extended states. It corresponds to an effective attraction between two localized electrons. The principle of a negative-U center is illustrated by having two centers which have a total of two electrons in their localized states. Electron-electron repulsion would have the electrons sit on different sites (b). However, structural relaxation would have them sit on the same site (a). The dominance of the latter is called a negative-U and corresponds to a localized pairing similar to the Cooper pairing of extended states in BCS superconductivity. Local pairing is common in defects in semiconductors.

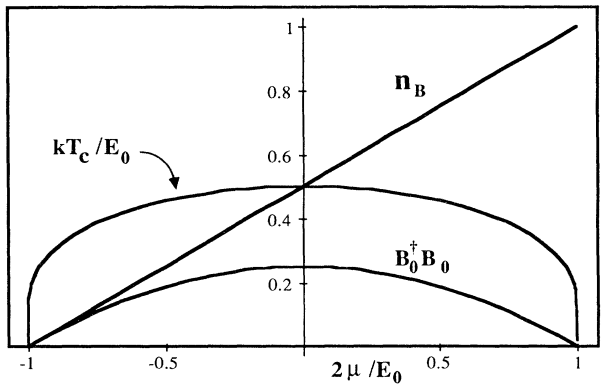

FIG. 6. Basic parameters in hard-core boson condensation on a lattice of paired sites [Fig. 5(a)]—negative-U lattice theory. The density of pairs on the lattice is given by n_B and is a linear function of the Fermi energy (μ). E_0, reflecting the boson mobility, is the half width of the boson band. $kT_c(\mu)/E_0=\lambda(\mu)$ is shown in mean-field theory and varies slowly near half-filling, which has the largest T_c with $\lambda(\mu)=\frac{1}{2}$. Below half-filling the condensation can be thought of as condensation of pairs, above half-filling as condensation of pair holes. The boson condensate at $T=0$ is $\langle B_0^\dagger B_0\rangle=Nn_B(1-n_B)$. In conventional negative-U lattice theory there is a competing charge-density-wave order because of nearest-neighbor repulsion. (Refs. 1 and 2). The effect of this repulsion is not included here since the hard-core boson model which results from the two-component theory does not intrinsically have the nearest-neighbor repulsion.

where $B_i^\dagger$ creates a pair on site i. Let E_0 be the energy of the zero-momentum boson, measured with respect to the average boson energy $E_q^0=\langle E_q\rangle$. Then the condensation temperature is given by $kT_0=\lambda(\mu)E_0$. In mean-field theory $\lambda(\mu)$ is plotted in Fig. 6. The highest T_c is for half-filling when $kT_c=E_0/2$. Near half-filling T_c is weakly dependent on μ.

Mobile states. The energy of mobile states as a function of crystal momentum is shown in Fig. 7(a). The high mobility is directly related to the wide range of energies (dispersion) as a function of momentum. The Fermi energy denotes the separation between filled states and empty states. There are two types of excitations, electrons above the Fermi energy and holes below the Fermi energy. In conventional BCS superconductivity, pairing is self-consistently generated by a weak attractive scattering potential between the mobile states, coupling electrons of momentum k with electrons of momentum $-k$. The elementary excitations (bogoliubons) are hybrid excitations of electrons at k with holes at $-k$, with unequal weight. This has the effect of creating a gap in the spectrum which can be most easily illustrated by measuring hole excitations upwards in energy and generating the excitation spectrum in Fig. 7(b).

Two components. The two-component theory is a coexistence of both kinds of states where the paired states by themselves are essentially immobile and the single-particle states are not pairing. Combining the two types of states, mobile and paired, Fig. 8(a) shows what happens without any hybridization. The paired states are located at a particular energy on this diagram because they

have very little mobility. The energy at which the paired states are shown is $\mu_B = E_B/2$. Where E_B is the electronic energy of a pair (boson). If we consider lowering the Fermi energy from μ_1 in Fig. 8(a), first the single-particle states will be emptied. When the Fermi energy reaches $\mu_2 = \mu_B$ the Fermi energy remains fixed (pinned) while the paired sites are emptied two electrons at a time, until all the paired sites are emptied. Then, moving the Fermi energy further continues to remove electrons from the single-particle states (μ_3). Since the pairs are immobile and the single-particle states have no pairing, this picture would not be superconducting.

Once the two types of states are coupled this diagram is no longer unique, since the effect of the coupling depends on the position of the Fermi energy itself. If the Fermi energy is far away from the two-particle transitions, they are either almost completely empty or almost completely filled. They will tend to have little effect on the properties of the system, giving rise to a small pairing field on the single-particle states which falls exponentially with the distance of the Fermi energy from the paired-state transition. The highest superconductive transition occurs when the Fermi energy is at half-filling of the bosonic states. The effect of the hybridization is shown in Fig. 8(b) where the boson band is half-filled. A gap opens up in the single-particle states, just as in BCS theory, except that here the gap is controlled by the hybridization w and the square root of boson condensate [which is $Nn_B(1-n_B)$ at $T=0$]. The bosons become mobile (dispersive) as reflected in the energy width of the boson band E_0. E_0, which controls the condensation temperature, is determined primarily by w, and the density of the single-particle states near the Fermi energy.

As the temperature is increased from $T=0$, bosons evaporate from the condensate and the fermionic gap Δ decreases. The boson energy width E_0 is temperature dependent, increasing slightly as Δ decreases, then decreasing again above T_c. The boson excitations coexist with fermionic excitations across the fermion gap. These fermionic excitations are coupled to the bosons leading to a hybridization of electrons with holes. Unlike BCS theory the hybridization is not only between electrons at k, with holes at $-k$ but with all holes, specifically the degenerate electron and hole at k and k' in Fig. 8(b). Because of this, at half-filling of the bosonic band long-lived fermionic excitations are neutral hybrids of electrons and holes. The onset of fermionic excitations is also significantly broadened. Before the condensate evapo-

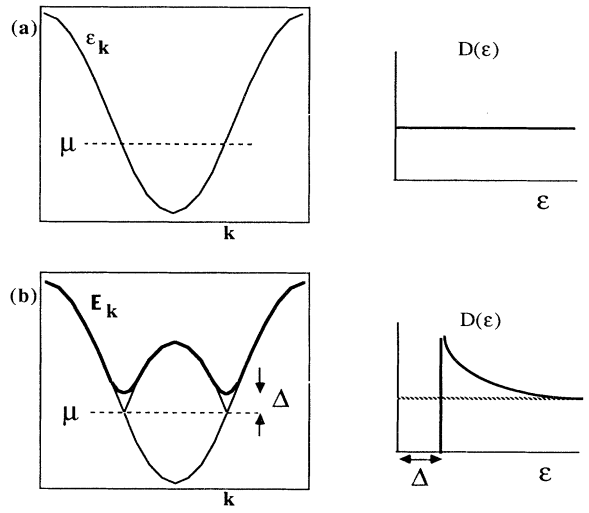

FIG. 7. (a) illustrates the mobile single-particle-state energy as a function of momentum. The energy (vertical) width of the band is proportional to the electron mobility. The Fermi energy separates filled states from empty states. Excitations are electronlike above the Fermi energy and holelike below the Fermi energy. The density of excitations near the Fermi energy is essentially constant as illustrated to the right. In the usual BCS superconductivity theory a weak attractive interaction gives rise to a pairing between electrons. The excitations are now mixed electrons and holes of momentum k and $-k$. To show the effect of hybridization it is convenient to measure both hole and electron excitations upwards from the Fermi energy as shown in (b). The hybridization results in an opening of a gap in the excitation spectrum wherever the Fermi energy lies as shown by the thick line, and to the right in the density of excitations near the Fermi energy. In the figure the typical scale of the gap ~ 0.001 eV is greatly exaggerated compared to typical bandwidths ~ 1 eV.

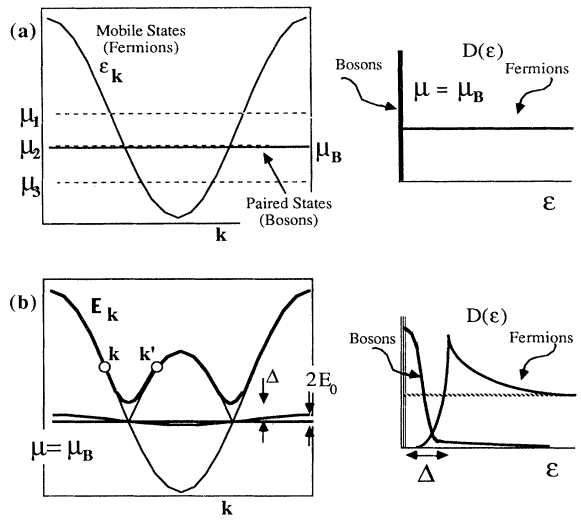

FIG. 8. The two components are combined, a mobile single-particle band as in Fig. 7(a) and a lattice of paired states with a transition energy $\mu_B = E_B/2$. The mobile states are assumed to have no intrinsic pairing and the paired states are assumed intrinsically immobile corresponding to no momentum dependence of their energy. Without hybridization between the two kinds of states there is no superconductivity (a). The occupation of the boson band depends on the Fermi energy. The effect of a small hybridization is illustrated in (b) for the case of half-filling of the boson band $\mu = \mu_B$ where the hybridization has its most dramatic effect on the properties of the material. The ability of mobile electrons to spend time on the paired sites and the paired electrons to spend time in the mobile states results in a gap opening in the mobile-state spectrum similar to the BCS theory [Fig. 7(b)], and the paired states gain mobility leading to superconductivity. The size of the gap is controlled by the boson (paired-state) condensate, T_c is controlled by the mobility of the bosons given by E_0 (Fig. 6). The density of excitations is illustrated to the right in the vicinity of the Fermi energy.

rates entirely, the boson condensate is able to scatter into the fermionic excitations, and true supercurrents no longer flow, leading to a resistive transition temperature T_c'. Then the condensate evaporates at a higher temperature T_c. Even when the condensate evaporates, because of the continued existence of the pairs, the resistive "normal" state has properties very different from a normal metal. At half-filling, current is carried by the charged $2e$ bosons rather than the neutral fermions.

Another way of illustrating the two-component theory is through Feynman diagrams showing particle processes. Figs. 9(a)–9(i) show some of the important diagrams in the two-component theory. The diagrams consist of single-particle propagators and paired propagators and are to be contrasted with the usual diagrams [Figs. 9(a')–9(g')] which describe fermion-boson interactions when the boson is a phonon. The diagrams are based on the vertex in Fig. 9(c) which is the conversion of two single particles into a pair (hopping to a localized state), or the conversion of a pair into two single particles (hopping from localized to extended states). Diagram 9(d) indicates the pairing of single particles. Diagram 9(e) indicates the movement of the paired particles. Diagram 9(f) indicates the process of an electron turning into a hole plus a pair and back—the self-energy diagram of the electron. The formal treatment of these diagrams does not make use of the usual boson propagator because the paired states are hard-core bosons. The diagrams represent directly the second-order expansion of the perturbation series of the hybridization w. Nonperturbative techniques, however, are to be used because all of these diagrams are infinite at $T=0$, because the two types of states, mobile and paired, coexist at the same energy. The single-particle diagram 9(f) continues to diverge in the normal state, indicating the need to hybridize electrons and holes, forming neutral excitations.

The response diagrams are indicated in Figs. 9(a)–9(i), where the particle-hole, paired particle-hole and pair-dissociation (or -formation) diagrams are to be considered as possible excitations. Neutrality of long-lived fermionic excitations at half-filling is important in determining the response.

B. Formalism

A Hamiltonian which embodies the features of the two-component theory is (in real and momentum space)

$$H=\sum_{i,\delta,\sigma} t_\delta c^\dagger_{i+\delta,\sigma}c_{i,\sigma}+E_B\sum_i B_i^\dagger B_i+\left[\sum_{i,\delta} w_\delta c^\dagger_{i+\delta,\uparrow}c^\dagger_{i+\delta,\downarrow}B_i+\text{H.c.}\right]$$
$$=\sum_{k,\sigma}\varepsilon_k c^\dagger_{k,\sigma}c_{k,\sigma}+E_B\sum_q B_q^\dagger B_q+\left[\frac{1}{\sqrt{N}}\sum_{q,k} w_q c^\dagger_{k,\uparrow}c^\dagger_{-k+q,\downarrow}B_q+\text{H.c.}\right],\quad w_q=\sum_\delta e^{iq\delta}w_\delta\ . \tag{2}$$

The mobile electrons are created by the fermion operators $c^\dagger_{i,\sigma}$. The paired states are formed out of two single-particle creation operators $B_i^\dagger=b^\dagger_{i,\uparrow}b^\dagger_{i,\downarrow}$. The energy of mobile states ε_k (Fig. 8) is related by Fourier transform to the single-particle hopping t_δ. The pairs have no intrinsic hopping, just an energy E_B. The hopping between paired and mobile bands is given by w_δ. The momentum dependence of w_q depends on the way pairs can hop onto single-particle states as shown in Figs. 3 and 4. If the single-particle states have a positive on site correlation energy then up and down electrons will hop onto a paired site from different original sites [Fig. 3(c)].

The formal treatment of the mixed fermion-boson system relies upon variational, mean-field, or perturbation treatment of the excitations so as to effectively decouple the two systems.

Several of the basic features of the phenomenology of this theory can be obtained using a BCS mean-field theory approach at $T=0$. The variational wave function is

$$\Psi=\prod_k(u_k+v_k c^\dagger_{k,\uparrow}c^\dagger_{-k,\downarrow})\prod_i(u_i+v_i B_i^\dagger)|0\rangle\ . \tag{3}$$

The first product is the usual BCS correlated wave function for the single-particle states with variables u_k, v_k. The second product is a similar product in real space which can be used to represent the ground state of the negative-U lattice with variables u_i, v_i. $v_i^2=n_B$ the pair site occupancy, and $u_i^2=1-v_i^2$. Another way to represent the mean-field ground state of the negative-U lattice is as a symmetric sum of all possible arrangements of pairs.

Above $T=0$, a Bogoliubov transformation of the single-particle states enables the single-particle states to be treated as a BCS superconductor with a gap. The effect of this transformation is to effectively decouple the two problems with a cross coupling only through the $q=0$ term and the order parameters. The transformation separates and treats exactly the dominant $q=0$ term in the coupling Hamiltonian. Since the boson condensate $\langle B_0^\dagger B_0\rangle$ is a macroscopic number B_0 and $B_0^\dagger$ are treated as numbers. The dispersion E_q of the bosonic excitations can be treated by perturbation theory of the $q\neq 0$ terms. The width of the bosonic band, E_0 can be obtained variationally by taking the derivative of the energy with respect to the boson condensate. This solution process leads to the above picture of elementary excitations—a fermionic gap with bosonic states inside the gap. It also provides expressions for the Bose condensate temperature, the fermionic gap, and the thermodynamic critical field. The effective decoupled Hamiltonian is written in the form

$$H-\mu N=\sum_k[(\bar{\varepsilon}_k-\mathsf{E}_k)+\mathsf{E}_k(\gamma^\dagger_{k0}\gamma_{k0}+\gamma^\dagger_{k1}\gamma_{k1})]+(\bar{E}_B-E_q^0)B_0^\dagger B_0+\sum_{q\neq 0}(\bar{E}_B+E_q)B_q^\dagger B_q\ ,$$
$$\mathsf{E}_k=[|\Delta(T)|^2+(\varepsilon_k-\mu)^2]^{1/2},\ \gamma_{k,\sigma}\text{ are bogoliubon operators}\ , \tag{4}$$

$$E_q \approx |w_q|^2 \tfrac{1}{2} \sum_k \left[1 + \frac{\bar{\varepsilon}_{q-k}}{\mathsf{E}_{q-k}} \frac{\bar{\varepsilon}_k}{\mathsf{E}_k} \right] \left[\frac{1}{\bar{E}_B - \mathsf{E}_k - \mathsf{E}_{q-k}} + \frac{1}{-\bar{E}_B - \mathsf{E}_k - \mathsf{E}_{q-k}} \right]$$
$$- \left[\frac{\bar{\varepsilon}_{q-k}}{\mathsf{E}_{q-k}} - \frac{\bar{\varepsilon}_k}{\mathsf{E}_k} \right] \left[\frac{1}{\bar{E}_B - \mathsf{E}_k - \mathsf{E}_{q-k}} - \frac{1}{-\bar{E}_B - \mathsf{E}_k - \mathsf{E}_{q-k}} \right] - E_q^0, \quad \bar{\varepsilon}_k = \varepsilon_k - \mu, \quad \bar{E}_B = E_B - 2\mu \ . \tag{5}$$

The first term in the sum over k is the ground-state energy. The second term is the energy of excitation of the single-particle states with the new dispersion E_k (bogoliubons). The bosons now have a momentum-dependent energy E_q. The $q=0$ term is buried in the ground-state energy term. E_q^0 is adjusted so that the average of E_q is zero. This is the action of a pair back onto itself which shifts E_B and is subtracted out from the q dependence of E_q and the condensation energy. Expressions for E_q are discussed below in the section on the coherence length. For $|E_B - 2\mu|$ greater than 2Δ the perturbation theory expression for E_q diverges in the limit $q \to 0$.

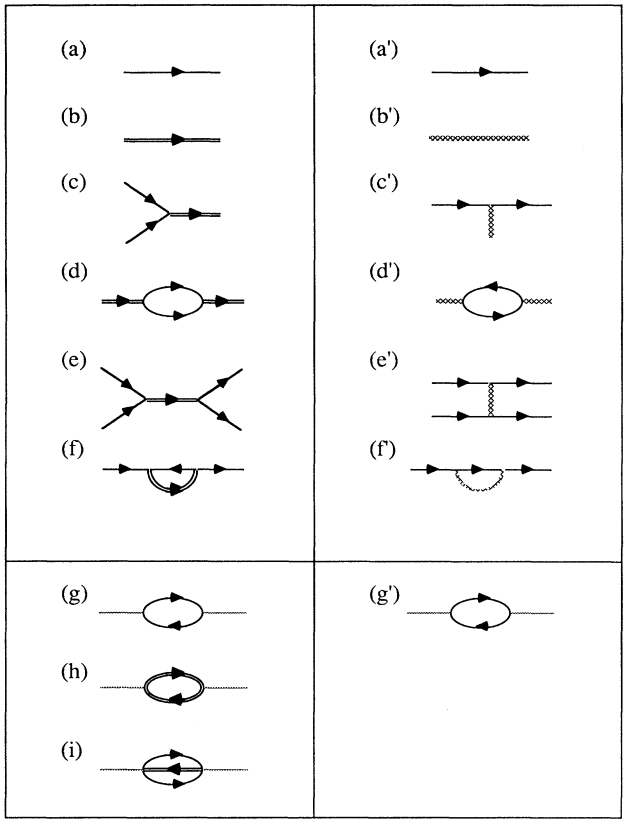

FIG. 9. Feynman diagrams (a)–(i) illustrating basic particle reactions of the two-component theory in contrast to the usual diagrams (a')–(g') of electrons interacting with bosons such as phonons or photons. A single particle (propagator) is illustrated by a single line with an arrow (a) and a pair by a double line with an arrow (b), the shaded line (b') is for a phonon or photon. Response diagrams for interaction with external fields have photon propagators (g)–(i) and (g'). The difference between these two sets of diagrams is essentially contained in the comparison of diagrams (c) and (c'), which shows that in the usual case an interaction, an emission or absorption of a boson conserves the electron. In the two-component theory two electrons convert into a pair, or are created by the decay of a pair. In (c') the $q=0$ boson state has no meaning, while in (c) it is the essential boson condensate. As explained in the text, it is useful to consider diagrams (d)–(f). The existence of fermionic states and bosonic states at the same energy, however, guarantees that these diagrams are divergent, so an essential part of the analysis relies on treating nonperturbatively the original reaction diagram (c).

The solution of the decoupled Hamiltonian follows from the finite-temperature behavior of the now dispersive boson system and the direct dependence of the fermionic gap on the boson condensate as discussed below (Sec. III A). Mean-field theory may be used for treating much of the finite-temperature behavior of the hard-core boson problem because the hopping through the single-particle states is further than nearest neighbor. This hopping translates into the coupling in the equivalent spin x-y model. In the standard treatment of the negative-U lattice problem, in addition to boson hopping there is a nearest-neighbor repulsion. This does not happen in the two-component theory because the hopping is indirect. For this reason, the present Hamiltonian is equivalent to an x-y model rather than the usual Heisenberg model.[1,2]

The effect of the $q \neq 0$ terms on the single-particle states has thus far been neglected. The primary effect is to hyridize electronlike bogoliubons with holelike bogoliubons at all energies and dramatically broaden the onset of the fermionic gap. The hybridization can be seen in the direct solution of small model problems. In the section on normal-state properties, a mean-field–random-phase approximation (RPA) solution of the fermionic elementary excitations at half-filling is discussed. The treatment is supported by commutators of the bosonic operators which have a zero expectation value implying that they may be treated in mean-field theory as number operators. A more detailed discussion of the RPA solution will be given elsewhere; it leads to neutral fermionic excitations and the broadening of the fermionic gap onset in the superconducting state.

III. PHENOMENOLOGY

A. The superconducting transition temperature and the fermionic gap: T_c, Δ

For comparison, the mean-field solution process for BCS theory and the two-component theory are contrasted pictorially in Figs. 10 and 11.

BCS theory. The electron-phonon interaction leads to a self-consistent pairing of electrons (Fig. 10) and a gap in the fermionic spectrum below T_c. Both T_c and $\Delta(T)$ are obtained from the self-consistent gap equation (shown for comparison with the two-component theory equations):

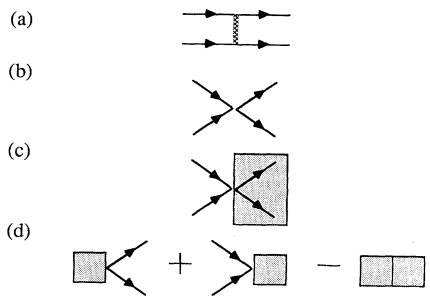

FIG. 10. Pictorial illustration of the conventional mean-field solution of BCS theory. The effect of electrons interacting through phonons (a) is assumed to collapse to an effective attractive scattering (b). The scattering is simplified by averaging separately incoming electrons and outgoing electrons illustrated by the shaded square in (c) which results in the diagrams of (d) which involve electron pairs annihilating or being created, or can be thought of as electrons converting into holes or into electrons. The average is the order parameter—the excitation spectrum gap Δ. Δ is zero in the normal state and nonzero in the superconducting state. Since these diagrams involve only one-particle processes they can be solved exactly by linear superposition of the electron and hole states (Bogoliubov transformation), creating a new single-particle states (bogoliuibons). The double shaded square in (d) indicates the need to subtract out the "overcounting" of the original diagram (b) by the two diagrams (d).

$$\text{(BCS)}\ \Delta=\frac{V}{N}\sum_k u_k v_k$$
$$=\frac{1}{2N}\sum_k \frac{V\Delta\tanh(\beta \mathsf{E}_\varepsilon)}{[\Delta^2+(\varepsilon_k-\mu)^2]^{1/2}}$$
$$=\Delta V\int_0^{\hbar\omega_D} d\varepsilon\, D(\varepsilon)\tanh(\beta \mathsf{E}_\varepsilon)/\mathsf{E}_\varepsilon\ ,$$
$$\mathsf{E}_\varepsilon=(\varepsilon^2+\Delta^2)^{1/2}\ . \quad (6)$$

V is the effective electron-electron attraction which is cut off at the Debye frequency $\hbar\omega_D$. $D(\varepsilon)$ is the density of electronic states for each spin. E_ε is the new excitation energy with the gap Δ. Δ can be canceled from both sides leaving the only dependence on Δ in the integrand. Evaluating the expression at $T=0$ gives an expression for $\Delta(T=0)$, and evaluating the same expression for $T=T_c$ where Δ becomes zero gives an expression for T_c. The two expressions (Table I) are related by a constant giving the relationship $2\Delta=3.5kT_c$.

Negative-U lattice theory. As described above (Fig. 6), the condensation transition for a negative-U lattice is controlled by the width of the boson band (mobility of the pairs) E_0:

$$\text{(negative-}U\text{ lattice)}\ kT_c=\lambda(\mu)E_0\ , \quad (7)$$

where $\lambda(\mu)$ is the Fermi-energy dependence shown in mean-field theory in Fig. 6. Since λ will be used to denote the mean-field result, the notation λ' will be used for the negative-U lattice when a precise value is needed (Table I).

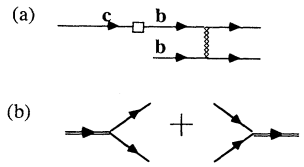

FIG. 11. Pictorial illustration of the mean-field solution of the two-component theory. Two types of electronic states exist in the material, one of which has a strong electron-phonon coupling (a) leading to immobile pairs. A small probability of conversion of c to b (or direct pair exchange) leads to the diagrams of (b). These diagrams are quite similar to the diagrams of BCS mean-field theory Fig. 10(d). The cases where no momentum is transferred to the paired states are exactly analogous to BCS theory diagrams in the condensed state and are treated similarly. Diagrams where momentum is transferred from or to the paired states are used to obtain the boson mobility, and a more complete hybridization of electrons and holes than exists in BCS theory. The absence of the overcounting diagram leads to a substantial difference in the condensation energy of the two theories.

Two-component theory. The mean-field two-component theory is quite similar to the BCS theory but the expressions are used quite differently. The gap equation is no longer directly self consistent. There are two cross-related "gap" equations for the fermionic gap Δ and for the boson order parameter Δ', which is not a gap (it is a local field). Self consistency is in two steps from fermions to bosons to fermions. Similar to BCS theory Δ is isotropic (s-wave superconductivity). The mean-field analysis leads to the following expressions at $T=0$:

$$\Delta=\Delta_k=-\frac{w}{N}\sum_i u_i v_i=-\frac{w}{2}\frac{\Delta'}{[\Delta'^2+(E_B/2-\mu)^2]^{1/2}}\ , \quad (8)$$

$$\Delta'=\Delta_i=-\frac{w}{N}\sum_k u_k v_k=-\frac{w}{2}\frac{1}{N}\sum_k\frac{\Delta}{[\Delta^2+(\varepsilon_k-\mu)^2]^{1/2}}$$
$$=-\frac{w}{2}\Delta\int d\varepsilon\, D_c(\varepsilon)/\mathsf{E}_\varepsilon\ .$$

TABLE I. Comparison of basic superconducting parameters for BCS theory of weakly paired mobile states, negative-U lattice theory of strong-pairing low-mobility states, and the two-component theory. At half-filling of the boson band $\lambda=0.5$, $\lambda'=0.3$, $\beta,\delta=1$, and $\delta'=1.6$. Expressions for λ,β,δ as a function of μ and explanations are given in the text.

	BCS	Negative-U lattice	Two-component
kT_c	$1.13\hbar\omega_D e^{-1/D(\mu)V}$	$\lambda'(\mu)E_0$	$\lambda(\mu)w^2D_c(\mu)\ln(1.13t/kT_c)$
Δ	$2\hbar\omega_D e^{-1/D(\mu)V}$		$\beta(\mu)w/2$
$\Omega_0H_c^2/8\pi$	$\Omega_0D(\mu)\Delta^2/2$	$\delta'(\mu)kT_c/2$	$\delta(\mu)kT_c/2$
$2\Delta/kT_c$	3.5		$4\beta/[\lambda w^2D_c(\mu)\ln(1.13t/kT_c)]$
ξ	$\hbar v_F/\pi\Delta$	a	$a<\xi<\hbar v_F/\pi\Delta$ (Fig. 14)

w is the zero-momentum hybridization of the paired and single-particle states $w_{q=0}$. The energy cutoff of Δ and the integral is the full single-particle band rather than $\hbar\omega_D$ as in BCS theory. A plot of the magnitude[46] of Δ, Δ', and E_0 at $T=0$ as a function of $\mu-\mu_B$ is given in Fig. 12 for the case of a constant single-particle density of states $D_c(\varepsilon)$ with parameters estimated for $YBa_2Cu_3O_7$ as given below. The assumption of a constant single-particle density of states $D_c(\varepsilon)$ is not as good for real systems as the same assumption for BCS theory because the integration cutoff is the full bandwidth.

For $T\neq 0$ a mean-field decoupling of the two components with the order parameters serving as the coupling leads to the expressions

$$
\begin{aligned}
&|\Delta(T)|^2 = w^2\langle B_0^\dagger B_0\rangle/N \ , \\
&\Delta'(T) = -\left\langle \frac{w}{N}\sum_k c_{k,\downarrow}c_{-k,\uparrow}\right\rangle \\
&\quad = -\frac{w}{2}\Delta(T)\int d\varepsilon\, D_c(\varepsilon)\tanh(\beta E_\varepsilon)/E_\varepsilon \ .
\end{aligned}
\tag{9}
$$

The fermion gap size Δ is explicitly given by the boson condensate. These equations give the mean fermionic gap because the coupling of the single-particle states to the $q\neq 0$ bosons gives a range of values of the fermionic gap, leading to lower and higher features in the excitation spectrum.

Unlike BCS theory, where Δ and T_c are determined by the same equation, T_c is determined by the energy width of the boson band like a bosonic system, generated, however, by the hopping of bosons through the single-particle states. The width of the boson band is determined variationally, $\delta\langle H\rangle/\delta\langle B_0^\dagger B_0\rangle$, below T_c. Near and above T_c perturbation theory also gives the same result [the electron-electron bubble Fig. 9(e)]:

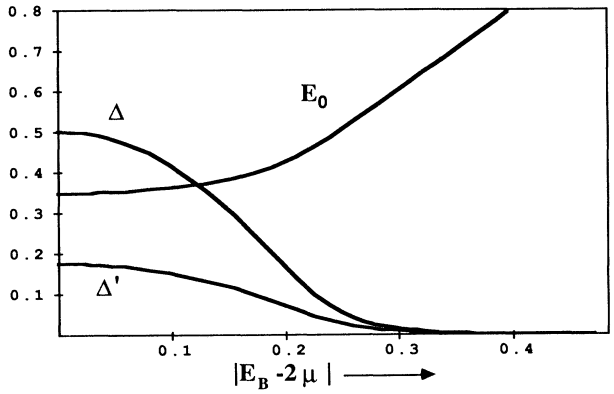

FIG. 12. Solution of the zero-temperature mean-field theory of the two-component theory for a constant single-particle density of states showing the two order parameters Δ (the mean fermionic gap) and Δ' and the superfluid dispersion width E_0 (without the shift E_q^0) as a function of $|E_B/2-\mu|$ (The distance of the Fermi energy from the uncoupled two-particle transition energy). Units of both axis are the coupling strength w. Δ and Δ' decay exponentially a distance of Δ' away from half-filling. T_c is determined from E_0 and Fig. 6. T_c is large only for a region of Fermi energies of order E_0, which is quite small. Experimentally, this does not require high precision to match since the Fermi energy is "pinned"—to shift the Fermi energy from half-filling a distance E_0 involves adding or subtracting one electron per unit cell.

$$
\begin{aligned}
&E_0(\mu) = w\Delta'(\mu)/\Delta(\mu) - E_q^0 = w^2 D_c(\mu)\ln[2t/\Delta(\mu)] - E_q^0, \quad T=0 \ , \\
&E_0(T) = w\Delta'(T)/\Delta(T) - E_q^0 = \begin{cases} w^2 D_c(\mu)\ln[2t/\Delta(T)] - E_q^0, & \Delta(T)\gg kT \\ w^2 D_c(\mu)\ln(1.13t/kT) - E_q^0, & \Delta(T)\ll kT \ . \end{cases}
\end{aligned}
\tag{10}
$$

The latter expressions assume an approximately constant density of states of width $2t$. The decoupled equations imply T_c is given by

$$
\begin{aligned}
&kT_c(\mu) = \lambda(\mu)E_0(\mu) \\
&\quad = \lambda(\mu)\{w^2 D_c(\mu)\ln[2t/kT_c(\mu)] - E_q^0\} \ , \\
&\lambda(\mu) = \tfrac{1}{2}(1-2n_B)/\tanh^{-1}(1-2n_B) \ , \\
&(1-2n_B) \sim (\mu-\mu_B)2/E_0(\mu) \ .
\end{aligned}
\tag{11}
$$

$\lambda(\mu)$ is given in mean-field theory (Fig. 6) which can be used because of the further than nearest-neighbor hopping. Because E_0 is temperature dependent, the expression is self-consistent with a weak logarithmic dependence on T_c itself. For half-filling of the boson band the expressions for Δ and T_c simplify [$\lambda(\mu)=0.5$] to

$$
\begin{aligned}
&\Delta = w/2 \\
&kT_c = (1/2)[w^2 D_c(\mu)\ln(2t/kT_c) - E_q^0]
\end{aligned}
\tag{12}
$$

Note that $2\Delta/kT_c$ is not universal.

A numerical comparison of these predictions can be made with experiments on 1:2:3:7 material using rough simplifying assumptions. The boson band is assumed to be at half-filling. E_q^0 is neglected. The native hopping of the paired band and the electron-electron interaction in the single-particle band are assumed unimportant. Then the predictions can be compared by making use of single-particle theoretical calculations of the bandwidth and density of states at the Fermi energy (Table II).[43] The value used for $D_c(\mu)$ involved subtracting out the contribution to $D(\mu)$ of the localized band, which are the paired states in this theory. Only one parameter remains unknown—w. w is set using the experimental value for $T_c=92$ K. The value of w that is obtained is 0.042 eV,

TABLE II. Model parameters from electron structure calculations (Ref. 31) and (T_c) from experiment, for use in comparison of theory with experiment.

Model parameters for $YBa_2Cu_3O_7$ (1:2:3)	
$D(\mu)$	2.75 electrons/eV cell spin
$D_c(\mu)$	1.7 electrons/eV cell spin
$2t$	3 eV
T_c	92 K

which is small, consistent with the assumptions of the theory. This value, and therefore of Δ is quite sensitive to the value used for $D_c(\mu)$. The measurement of Δ (or $2\Delta/kT_c$) then provides an experimental test of the theory. The theoretically predicted value of $2\Delta/kT_c$ is 5.3. This value is somewhat larger than the BCS value 3.5, however, in the two-component theory there is no guarantee that this number should be near any particular value. Experimentally,[47–53] values from different types of measurements have given a wide range of values from 0 to 8 (even no gap has been reported). Within the context of the simplifying assumptions, since the value predicted by two-component theory is within reasonable range of the experimental values, this is encouraging.

Moreover, within the two-component theory it is possible to suggest why different experiments give different values of the gap. The existence of two different components suggests a more complicated response of the material particularly since E_0 and Δ are of the same order. The spreading of the onset of fermionic excitations further complicates the excitation spectrum. At bosonic half-filling the neutrality of the fermionic excitations implies that vanishing or near-vanishing matrix elements affect some response functions. Some evidence for a splitting of gap features exists from tunneling data.[52,53] It is significant to note that data on infrared (ir) reflectivity[49,50] has been interpreted in two different ways to yield the values 3.5 and 8. These two interpretations look specifically for signatures of the lowest gap and of the highest gap. This is consistent with the development of lower and upper fermionic gaps through single-particle hybridization from the theoretical mean gap 5.3. It also contradicts the usual assumptions that either the largest or the smallest gap size measured should be considered most definitive. Above T_c the hybridization of electrons and holes leads to a region in the vicinity of the Fermi energy where the occupation of electronic states is different from the conventional occupation. Experiments[51] which observe a persistence of gaplike signatures into the normal state are likely to be sensitive to matrix elements affected by this change in occupation. A qualitative difference in behavior between different samples can also be understood in this context since in samples not at half-filling the fermions are charged. Systematic variations in Δ and T_c also occur and these variations are discussed in more detail in the companion article discussing more direct application to Cu-O-based superconductors.

In the two-component theory, within the fermionic gap Δ there are present bosonic excitations which should affect a variety of response functions. A significant body of experimental evidence exists for the presence of excitations within the measured gap.[53,54] Direct observation of boson-pair excitations should be possible. The boson dispersion (Fig. 13) suggests a dominance of large momentum excitations or phononlike absorption in infrared and Raman spectroscopies. The half width of the boson band with respect to its average energy is $E_0=2kT_c$, which for 1:2:3:7 material is 0.015 eV or 120 cm^{-1}. Since boson pairs must be excited, the expected excitation peaks (more than one for a noncubic material) are around $2E_0=240$ cm^{-1} and may be as high as $4E_0$, which coincides with a region of large phononlike absorption peaks with anomalous temperature dependences in experiment.[47,50]

Subtleties occur in the vicinity of T_c. Because the fermionic gap is closing, there may occur mixing (scattering) of the boson condensate below the temperature of boson condensation T_c. The scattering leads to resistance.[55] Thus the superconducting-to-normal transition T_c' occurs below the thermodynamic transition T_c when the condensate disappears. A breakdown of perturbation theory suggests T_c' is determined by $|\mu_B-\mu|=2|\Delta(T_c')|$, implying that T_c-T_c' increases away from bosonic half-filling. The fermionic gap broadening (which increases near T_c) implies that scattering of the condensate before evaporation occurs even when $|\mu_B-\mu|=0$. The amount of the preemption would be expected to be small because the gap decreases rapidly only quite near to T_c. Anything which couples to the single-particle state energies such as disorder or a magnetic field further reduces T_c', broadening the resistive transition.

Experimentally, a broadening in the superconductive-to-resistive transitions is observed even in the best materials. The original explanation for this effect was sample inhomogeneity. It is tempting to conclude that this broadening is due in part to the difference between T_c', which denotes the onset of resistance due to condensate

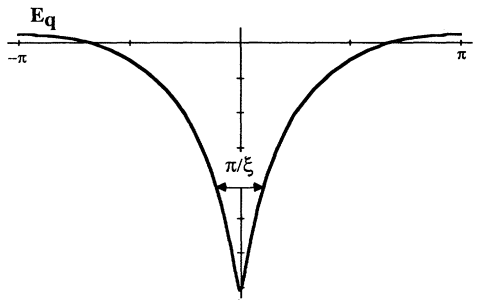

FIG. 13. Momentum dependence of the boson energy at $T=0$ due to the coupling between paired and mobile states as obtained from perturbation theory for a constant density of single particle states. Without any gap in the single-particle-state spectrum there is a weak logarithmic divergence at $q=0$. An approximate (BCS) form of the cutoff was used to generate this figure. The approximate coherence length is indicated.

scattering, and T_c, which denotes the disappearance of the superfluid. The broadening changes with doping with the narrowest transition at the highest T_c,[56] and systematic broadening occurs in a magnetic field,[57,58] consistent with this interpretation.

The s-wave nature of the superconductivity is consistent with experiment.[59,60]

B. The critical field H_c

The thermodynamic critical field H_c is the magnetic field which is capable of turning off the superconductivity. This corresponds to having an energy density $H_c^2/8\pi$ equal to the condensation energy ΔF.

BCS theory. Self-consistency leads to a first-order cancellation in the condensation energy as can be seen in the overcounting correction in Fig. 10(d). It then becomes second order in the gap or transition temperature.

$$\text{(BCS) } H_c^2/8\pi = D(\mu)\Delta^2/2 = 1.56 D(\mu)(kT_c)^2 \ . \tag{13}$$

Negative-U lattice theory. The condensation energy has no cancellation and is (per unit cell Ω_0)

$$\text{(negative-U lattice) } (H_c^2/8\pi)\Omega_0 = kT_c n_B(1-n_B)/\lambda \ , \tag{14}$$

$$\text{(negative-}U\text{ lattice at half-filling)} \sim 0.82 kT_c \ .$$

For a negative-U lattice theory only nearest-neighbor hopping can be allowed because the hopping is suppressed exponentially. Thus, for the latter expression at half-filling, λ has been taken for nearest-neighbor interactions on a cubic lattice where fluctuations reduce λ from the mean-field value 0.5 to 0.3 ($=\lambda'$).[61]

Two-component theory. Since the self-consistency is not direct, there is some cancellation, but the condensation energy of preformed pairs remains first order in kT_c. The absence of cancellation can be seen in the constant term of the Hamiltonian in Eq. (2), and in the diagrams of Fig. 11(b). Assuming that the H_c has the effect of removing all correlations, ΔF is the difference between the ground-state energy with the coupling w and without w (except for the self-action E_q^0, which is not sensitive to turning on the field) at $T=0$.

At half-filling the condensation energy per unit cell is $\Omega_0 H_c^2/8\pi = E_0/4$. This then gives a particularly simple relationship between the critical field and the critical temperature:

$$\Omega_0 H_c^2/8\pi = E_0/4 = kT_c/4\lambda \sim kT_c/2 \ , \tag{15}$$

Since this expression is relatively insensitive to details of the theory but is significantly different from the BCS phenomenology, it provides a good opportunity for comparisons of theory and experiment.

At half-filling there is no Fermi-energy shift when turning off w. Away from half-filling there is a Fermi-energy shift. Assuming the boson band is at least partially filled, then the Fermi energy with $w=0$ is just μ_B. If the boson band is less than half-filled, as w is turned on the Fermi energy shifts down, transferring fermions to bosons, increasing slightly the boson condensate. The opposite occurs if the boson band is more than half-filled and the pair holes are the active species:

$$H_c^2/8\pi\Omega_0 = \langle H \rangle_w - \langle H \rangle_{w=0}$$
$$= E_0(T=0)(\Delta'/w)^2 + (\mu-\mu_B)^2 D_c(\mu) \ . \tag{16}$$

A comparison can be made between BCS theory, two-component theory, and the negative-U lattice theory on the value of the energy density of the thermodynamic field. There are difficulties in obtaining an experimental value for H_c. In a small coherence length (type-II) superconductor obtaining H_c involves the geometric mean of two critical fields $H_{c1}(T=0)$ for flux penetration, and $H_{c2}(T=0)$ for the disappearance of superconductivity, including the effects of asymmetry, and an uncertain extrapolation of $H_{c2}(T)$ to $T=0$, since $H_{c2}(T=0)$ is too large to measure directly. Furthermore, the observed broadening of the resistive transition T_c-T_c' affects the determination of H_{c2}, and the nature of the short-range correlation function (Sec. III C) affects the interpretation of H_{c1}. This limits the conclusions which can be extracted until more systematic comparisons can be made. The energy density per unit cell for the three theories are given in Table III. A range of experimental results is indicated.[48,52] It has been generally stated that values of H_c measured in this family of materials are much larger than would be expected from BCS theory, consistent with the qualitative predictions of two-component theory. Since this is a qualitative difference between the two-component theory and any particle exchange theories (phonon or other), more comparisons with experiment should prove useful.

C. The coherence length ξ

The coherence length is the distance over which superconductivity (the gap Δ) recovers if suppressed locally or at a boundary, at $T=0$.

BCS theory. The recovery of superconductivity follows essentially a simple exponential form with decay constant

$$\text{(BCS) } \xi = \hbar v_F/\pi\Delta \ . \tag{17}$$

Negative-U lattice theory. As is expected from a nearest-neighbor interaction Hamiltonian the recovery distance is just a nearest-neighbor distance in the negative-U lattice.

Two-component theory. In two-component theory it is possible to ask two questions, one related to the behavior of superconductivity at a boundary between a two-component system and a normal metal where superconductivity decays because of lack of locally paired states beyond the boundary. The second is the recovery of superconductivity if it is suppressed within the two-component system. The former should display a hybrid behavior where the normal metal, superconducting by a

TABLE III. Comparison of theoretical and experimental values for 1:2:3 material using a number of simplifying assumptions (see text) and Table II. The one unknown parameter for two-component theory w is fit to T_c yielding the value $w \approx 0.042$ eV. The coherence lengths are given in units of the in plane lattice constant a and the interlayer separation d_z, $a \approx d_z = 3.9$ Å. The condensation energy per unit cell ($\Omega_0 H_c^2/8\pi$) is given in units of temperature.

	BCS	Negative-U lattice	Two-component theory	Experiment
$2\Delta/kT_c$	3.5		5.3	2.5–8
$\Omega_0 H_c^2/8\pi/k$	3 K	76 K	46 K	(9–36 K)[a]
ξ_{ab}	$25a$	$1a$[b]	(Fig. 14)	5–$9a$
ξ_z	?	$3d_z$[b]	$1d_z$	0.75–$1.8d_z$

[a]The parentheses around experimental values for the condensation energy indicates large uncertainty in its extraction from experimental results (see text).

[b]The negative-U lattice coherence assumes a nearest-neighbor interaction negative-U lattice coincident with the oxygen vacancies.

proximity effect, displays a BCS behavior with the BCS decay constant. Decay within the two-component system involves an interplay between the two kinds of states.

Within the two-component system, local pairing is determined by the paired states. The coherence and the order parameter are determined by the hopping of pairs through the single-particle states. This hopping describes the distance over which superconductivity is affected if it is suppressed locally. It is important to recognize, unlike a simple negative-U lattice theory, the coherence length is larger than the nearest-neighbor distance because the hopping proceeds through extended single-particle states, and is not exponentially suppressed on the negative-U states. The hopping probability T_δ is related by Fourier transform to the dispersion E_q of the bosonic states (Fig. 13). The width of the dip in the dispersion is reciprocal to the coherence length ξ. In perturbation theory, at $T=0$ the dispersion E_q is given at bosonic half-filling by

$$E_q = -|w_q|^2 \sum_k \left[1+\frac{\bar{\varepsilon}_{q-k}}{E_{q-k}}\frac{\bar{\varepsilon}_k}{E_k}\right]\left[\frac{1}{E_k+E_{q-k}}\right], \qquad T_R = \frac{1}{N}\sum_q e^{-iR\cdot q}E_q \ . \tag{18}$$

The coherence decay function is obtained by correcting T_R for volume factors by $J(R) \sim R^2 T_R$. The behavior of this expression is illustrated in Fig. 14. T_R decays as R^{-3} so $J(R)$ decays as a power law R^{-1}, and is cut off at a distance which, up to a numerical factor, is the BCS coherence length $\hbar v_F/\pi\Delta$. Without the cutoff, integrating over T_R to give E_0 would be logarithmically divergent. This logarithm is the same one which appears in the expressions for E_0 given above [Eq. (10)] where the logarithmic divergence is cutoff by Δ or T. Because of the power-law decay, the coherence length is lower than the BCS value, but larger than nearest neighbor. The power-law decay should be manifest in experiment in a "softness" of the coherence length and the experimental values should be somewhat dependent on the particular measurement made.

In 1:2:3:7 material there is a basic difference between the coupling in the x-y direction and the z direction. In the z direction ε_k are relatively constant (the fermions are assumed to hop weakly across the insulating layers). The q dependence of E_q arises from the pair hopping w_q (Fig. 3) and is therefore expected to have a coherence length comparable to the distance between the paired states and the complete Cu-O planes (Fig. 1). This is the interplanar separation $d_z = 3.9$ Å. In the x-y direction, coherence is controlled by the hopping of pairs as described above; the decay is given by Fig. 14. Experimental values[62–64] for the coherence length in the z direction are in the range 3–7 Å and in the x-y plane are in the range 16–34 Å corresponding to 5–9 lattice constants as shown in Fig. 14. These results are in essential agreement with the theoretical predictions.

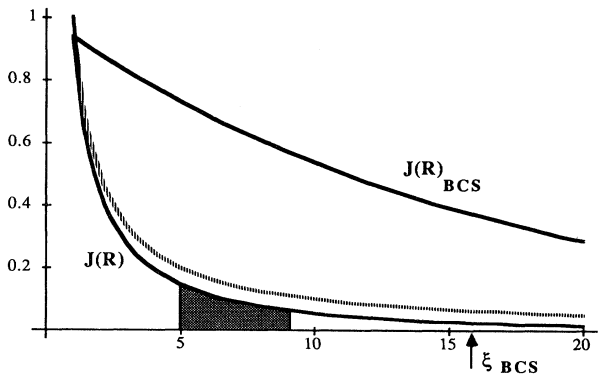

FIG. 14. The hopping range of the bosons gives the coherence length behavior of the superconductivity. The BCS exponential range function $J(R)$ with a coherence length based on material parameters is shown along with the power law (R^{-1}) decay of the two-component theory. The pure power-law decay (dashed line) is cut off in an approximate way using the exponential BCS range function. Experimental values for the coherence length in 1:2:3:7 material are indicated in the shaded region. The units of the horizontal axis are lattice constants $a = 3.9$ Å. The BCS decay length indicated differs from that in Table III since here the form of the decay uses the length appropriate to the gap of two-component theory.

D. Long-wavelength collective excitations

An important qualitative distinction exists in the long-wavelength collective modes between BCS theory, negative-U lattice theory, and their combination in a two-component theory. The properties of long-wavelength excitations in these theories are dealt with separately from the usual model Hamiltonians because these Hamiltonians do not contain the long-range Coulomb potential.

BCS theory. The long-wave collective high-frequency plasmon (charge-density wave) excitations in the BCS theory are high-frequency modes essentially the same as in a normal metal.

Negative-U lattice. The long-wave $q \rightarrow 0$ bosonic excitations in the negative-U lattice are themselves the charge-density waves. This is the plasmon whose excitation energy is very large. Thus the long-range Coulomb interaction should play an important role in a full treatment of the negative-U lattice theory; this has been largely untreated.

Two-component theory. The long-wavelength bosonic excitations in the two-component theory are *coupled* charge-density waves, where the charge oscillates between the single-particle and paired states. This corresponds to a screened plasmon of both the negative-U lattice and the mobile states. Since long-range displacements of charge are not involved, the long-range Coulomb potential in the Hamiltonian and the plasma frequency do not affect the low-energy modes. Since the dispersion is controlled by the mobile states, the long-wavelength boson essentially corresponds to a zero-sound wave in a neutral (screened) Fermi gas.[65] The zero sound in a neutral Fermi system is the analog of the plasmon in a charged Fermi system, and has a linear dispersion at $q \rightarrow 0$.

The other collective long-wave excitation, the acoustic phonon (sound waves), couples directly to the electronic long-wave boson excitation. The primary reason for this coupling is that E_B typically varies linearly with pressure through the pressure dependence of the local structure in the negative-U center. A second reason is a change in w with pressure. Thus hydrostatic pressure should affect superconductivity, and bulk modulii and sound waves should be affected by boson condensation.

A linear change in E_B with pressure implies that pressure affects the bosonic occupation similar to doping. The boson occupation, as has been discussed, affects all of the essential properties of superconductivity in a systematic way. The most observable effects are on T_c. Consider the case of a linear raising of E_B with pressure. If the Fermi energy is above boson half-filling, pressure increases the bosonic filling, raising T_c. If the Fermi energy is at boson half-filling very little effect should be observed, while if the Fermi energy is below boson half-filling T_c is lowered. The effect of changes in w with pressure is a systematic shift in these properties so that the turning point from raising T_c to lowering T_c is shifted slightly from boson half-filling.

Evidence in support of these predictions exists. Experimental observations support a pressure sensitivity which varies with doping.[66–68] Large anomalies in bulk moduli, sound waves, and internal friction have been found at the superconductive transition.[69–72]

E. The uncondensed "normal" state

The uncondensed state of the two-component theory does not behave as a normal metal because of the presence of paired states. Local pairing and its influence on the single-particle states remain even after evaporation of the condensate. The long-range coherence disappears, local coherence imposed by the large paring energy remains. The essential physical process is the local transition from single-particle to paired states. Rather than a normal system the behavior is of an evaporated soup of the elementary excitations of the superconducting state. Direct considerations suggest that the transport is dominated by charged bosons (paired states) while the fermionic excitations are neutral at half-filling of the boson band.

The importance of the coupling is revealed in the divergence of the single-particle self-energy diagram in Fig. 9(f). This diagram represents the process of an electron turning into a hole plus a pair. At half-filling of the boson band, these two states have the same energy. The coupling of two degenerate states, electron and hole, by the Hamiltonian implies that these states hybridize, with equal weight. This is due to the Hamiltonian term

$$w_{k+k'} c^{\dagger}_{k,\uparrow} c^{\dagger}_{k',\downarrow} B_{k+k'} , \tag{19}$$

which converts a hole at k' into an electron at k, where k and k' are related to each other as in Fig. 8(b). The change in boson number during this process is accounted for in the coherent ground state which does not conserve boson number at $k+k'$. In mean field at half-filling the boson operators may be treated as numbers because the expectation value of their commutators are zero:

$$\langle [B_q, B^{\dagger}_{q'}] \rangle = \langle \delta_{q,q'} - 2n_B(q-q') \rangle = 0 \quad \text{(at half-filling)} , \tag{20}$$

where $n_B(q-q')$ is the pair Fourier density operator. More generally, the $q \neq 0$ terms in the Hamiltonian couple all single-particle states, both electrons and holes. Wave packets which can couple to the local order (coherence) should be generated and they, in turn, induce local correlation (hopping) in the bosonic system.

The hybrid electron-hole fermion elementary excitations are neutral at half-filling for all electron energies. In contrast, in BCS theory electrons and holes hybridize *below* T_c but they have equal weight only for the electrons and holes originally at the Fermi energy. Unlike the fermion diagram, the bosonic diagram is convergent with the logarithmic divergence cut off by kT. The normal state is thus seen to be composed of neutral fermion and charged boson elementary excitations.

The neutrality of the fermionic excitations is not exclusive to the normal state, but extends throughout the superconducting state. The hybridization is stronger at higher temperatures because the bosonic states are mostly responsible for hybridizing k and $-k$ in the conden-

sate. At $T=0$ the hybridization is thus likely to be more easily broken.

Neutral fermion excitations and charged boson excitations lead to dramatic transport properties of the normal state. Since fermions are neutral, charged bosons carry current in the uncondensed state. Thus while fermions originally provide the mobility, the bosons carry the current once hybridization has been made. Without a complete solution of the normal state, transport is tentatively extracted from the boson properties as described by Fig. 9(d). The real part of this propagator has determined T_c. The imaginary part is the decay of a pair [Fig. 9(c)] which determines the boson lifetime. The q averaged imaginary part of the propagator is shown in Fig. 15 as a function of energy measured from the Fermi energy. Away from the Fermi energy the decay increases linearly with energy. For an approximately constant single-particle density of states,

$$\langle \mathrm{Im}\Sigma_B(E,q)\rangle_q = 2\pi w^2 D_c^2 E \coth[\beta E/2] , \quad (21)$$

where E is measured with respect to 2μ and $\beta \equiv (kT)^{-1}$. The reason for the linear dependence of the decay rate of the bosons into two single-particle states is illustrated in Fig. 16. Considering the decay of a boson at an energy E, it can decay into two electrons of energy $E/2$ or one of the electrons can have less energy and the other one more. Ultimately, the largest energy difference between the two electrons is just E since the low-energy electron cannot have an energy lower than the Fermi energy below which the electronic states are filled. The number of possible ways to decay is then just proportional to the energy E giving the dependence of Fig. 15. The decay rate of the boson at the Fermi energy ($E=0$) is proportional to kT. This is determined by the density of available fermion states at the Fermi energy, which is given by the range of energies (kT) where electronic states are partially occupied.

This derivation of the boson lifetime does not include some of the subtleties of this many-body problem. Since it is essentially based on phase space considerations the result is likely to continue to hold for more complete treatments.

Resistance. The Drude conductivity is given by

$$\sigma = (ne^2/m)\tau , \quad (22)$$

where n is the density, e is the charge, m is the mass, and τ is the lifetime of the charged particle. The lifetime refers to the scattering of a single particle. In this case the lifetime is determined by a decay of a paired state. The temperature dependence of this expression can be obtained assuming that n and m are independent of temperature, n because the pair density is determined by μ and is pinned by the large density of paired states, and m because m is controlled by the boson hopping range which is (aside from at most logarithmic factors) independent of temperature. τ is inversely proportional to the decay rate, which at the Fermi energy is $\langle \mathrm{Im}\Sigma_B(0,q)\rangle_q = 4\pi w^2 D_c^2 kT$. Thus the resistance $R \sim 1/\sigma$ is proportional to kT. This is illustrated in Fig. 17. Such a linear resistance has been measured in several of the high-T_c superconductors and is considered by many to be a signature of this form of superconductivity. Substantially away from half-filling, it is to be expected that a usual fermionic dependence of the resistance should be observed.

The frequency-dependent resistance

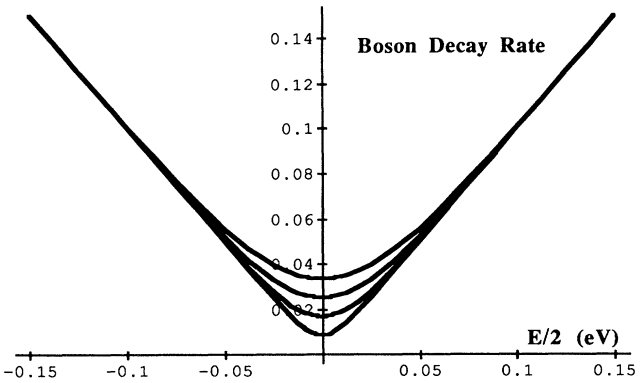

FIG. 15. The decay rate (inverse lifetime) of bosonic pairs in the uncondensed state at an energy E away from the Fermi energy. The function plotted is $g(x)=x\coth(x/kT)$ where the inverse lifetime $\langle \mathrm{Im}\Sigma_B(E,q)\rangle_q = 4\pi w^2 D_c^2 g(E/2)$. The axes are in electron volts. In $YBa_2Cu_3O_7$ the prefactor has the estimated dimensionless value 0.06. Four curves are plotted for different temperatures (from lower to higher) 100, 200, 300, and 400 K. The decay rate at the Fermi energy is proportional to the temperature; this leads to a linear resistivity (Fig. 17). Away from the Fermi energy the decay rate is proportional to $|E|$. This leads to the unusual behavior of the tunneling conductance (Fig. 19). The shape of the boson decay rate is due to phase space considerations illustrated in Fig. 16.

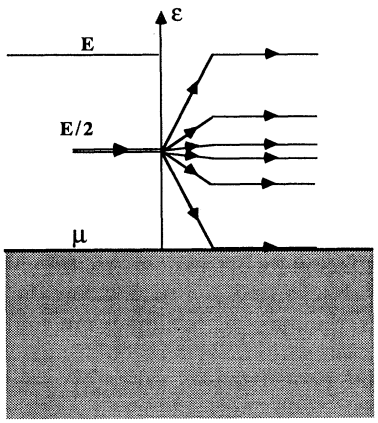

FIG. 16. Illustration of the processes by which a bosonic pair with energy E with respect to the Fermi energy can decay into two single-particle states. The pair (coming from the left) shown at the energy $E/2$ per electron can decay into two electrons at $E/2$, or one electron can have less and the other more energy. The limit in the difference between the energy of the electrons E is established by the Fermi energy below which the electronic states are filled. The number of ways the decay is possible (the phase space) is thus proportional to E giving rise to Fig. 15.

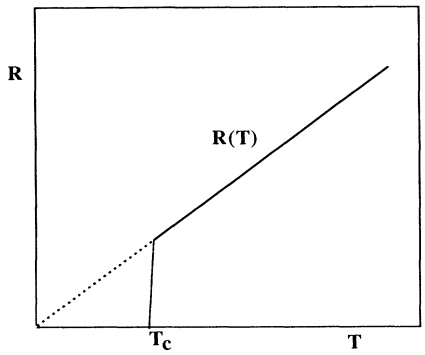

FIG. 17. Schematic illustration of the linear resistance in the uncondensed state obtained from the two-component theory. Such curves are believed by many to be characteristic of the high-T_c family of superconductors. Note that the two-component theory suggests that sufficiently away from half-filling (away from optimal superconductivity) the curve will be substantially different.

$$\sigma(\omega)=\sigma/(1+i\omega\tau)=(ne^2/m)\tau/[1+(\omega\tau)^2]$$

can also be obtained from these results using the frequency-dependent lifetime

$$\tau(\omega)\sim 1/4\pi w^2 D_c^2 \omega \coth[\beta h\omega/2] ,$$

which decreases as a function of ω, increasing the high-frequency tail of $\sigma(\omega)$. Such a frequency dependence has been suggested experimentally.[73]

Evidence for the importance of a narrow band in transport has been derived from a range of experimental results.[74] Sum rules of the conductivity which give estimates of n/m also give values much smaller than would be expected from the single-particle states.[75] This is consistent with the picture of neutral fermions and narrow-band charged boson transport.

Tunneling. In a tunneling process between a BCS superconductor and a metal through an insulating layer, the tunneling is controlled by the density of states of the superconductor. Above T_c this is constant, below T_c a gap opens up and the tunneling at $T=0$ is zero up to the gap width.

The tunneling current of electrons from a two-component material into a normal metal involves charged pairs of the two-component material decaying into the single-particle states of the normal metal. Thus the tunneling involves directly the decay process of Fig. 9(c). In order to understand how this decay process applies, the following discussion indicates that the properties of the interface itself enter. In Fig. 18 the interface is shown schematically for a narrow insulating layer. The applied voltage (V) which causes the tunneling current to flow means that the Fermi energy is lower in the metal than in the two-component material. Since the Fermi energy bends at the interface, the "pinning" of the Fermi energy by the paired band causes the band itself to bend (due to charge accumulation at the interface). The tunneling current is the combined decay of paired states into single-particle states. Tunneling data is usually expressed in terms of the conductance G, which is the derivative of

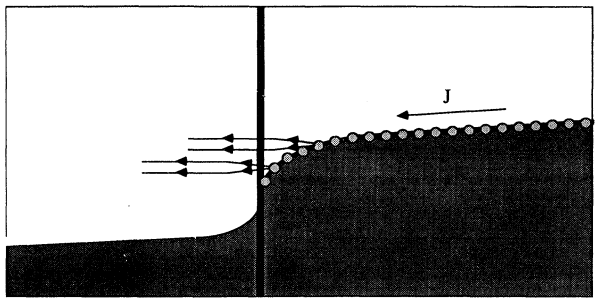

FIG. 18. Schematic illustration of a thin interface between a normal metal and a two-component material in the uncondensed state. The shaded region represents the occupied electronic states and the unshaded region the empty electronic states. The Fermi energy separates them. Current flows due to an applied voltage corresponding to the Fermi energy drop from right to left.

the current with respect to the applied voltage. This is the current due to small additional lowering of the Fermi energy in the normal metal. If the bosonic band does not bend at the interface, the change in V would raise the effective E of the paired states compared to the Fermi energy in the normal metal. This would give rise to a linear increase in boson decay rate (current) and a constant $G(V)$. In contrast, for a vertical arrangement of paired states, the change in V results in the *addition* of a paired state at V corresponding to $G(V)\sim\langle \mathrm{Im}\Sigma_B(V,q)\rangle_q$. Assuming that the actual bending of the paired band can be decomposed as a sum of these two contributions leads to $G(V)\sim G_0+\langle \mathrm{Im}\Sigma_B(V,q)\rangle_q$. The experimental results[53] on tunneling for different temperatures in the normal state of 1:2:3:7 material are quite similar to the theoretical curves in Fig. 15 as shown in Fig. 19. A sensitivity of these tunneling experiments to surface conditions is reasonable since it depends on the localized states and their hybridization near the interface.

Below T_c tunneling is affected by three changes. First, the averaging over q used in obtaining the decay characteristics above T_c should no longer apply, and tunneling is similar to a diffraction experiment where a structure factor leads to peaks in the tunneling data. In an experiment this is averaged over several crystallographic directions. Second, the single-particle states have a gap which is multistaged, affecting the decay probability and tunneling near the Fermi energy. Third, the condensation in the superconducting state inhibits the bending of the paired states, which is then possible only within a coherence length of the interface. Pair decay from the paired states into the normal metal is still possible at $V=0$ and $T<T_c$. This is consistent with the experimental zero-field conductance.[53] Experiments[53] which rule out pair-to-pair hopping across the interface, do not rule out pair *decay* which is responsible for tunneling at a two-component/metal interface.

F. Isotope shift and structural coherence

One of the central signatures of BCS theory is the isotope shift of T_c, since, in BCS theory,

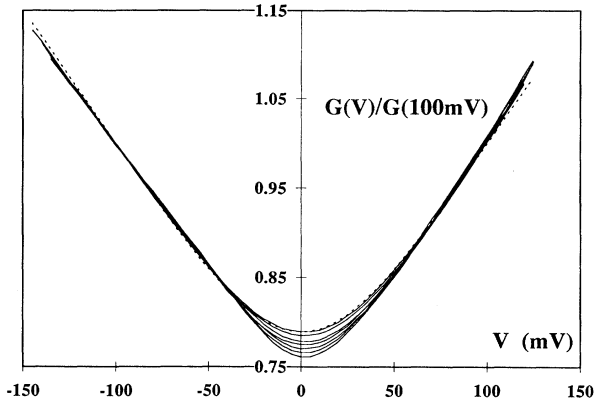

FIG. 19. Distinctive experimental tunneling conductance in the normal state of 1:2:3:7 material. Temperatures of the plotted curves are 100, 110, 120, 130, 140, 150, 169, and 180 K from bottom to top. Variation with V and T is given correctly by the pair lifetime (Fig. 15). The dashed line is the theoretical result of Fig. 15 with $T=180$ K and offset to the experimental data: $G(V)\sim G_0+\langle \mathrm{Im}\Sigma_B(E,q)\rangle_q$. A small asymmetry in the experimental data may be due to a shift of the Fermi energy away from bosonic half-filling and/or an energy dependence in the single-particle density of states. The data is normalized since prefactors or G_0 are weak functions of temperature (not shown). Data by courtesy of J. M. Vales, Jr., and M. Gurvitch and their collaborators (Ref. 53).

$T_c\sim\omega_D=(\kappa/M)^{1/2}$, where κ is the oscillator restoring force and M is the mass of atoms associated with the phonon responsible for the superconductivity. The isotope shift parameter $\alpha=-M/T\,dT/dM=\frac{1}{2}$.

In the two-component theory the isotope shift arises because of the internal workings of the negative-U center. This is implicit in the Hamiltonian used to obtain most of the above results. The following general considerations indicate that the isotope shift is sensitive to comparisons between different relaxation rates, structural and electronic, and should be small.

There are two electronic states of the negative-U center [Fig. 5(a)], unoccupied and doubly occupied. These also correspond to two different positions of nuclei (Fig. 20). A transition between the electronic occupations is accompanied by a shift in positions of the nuclei; this structural change is responsible for the negative U. The zero-point motion of the nuclei correspond to Gaussian wave packets in potential wells which are in first-order harmonic. The transition matrix element w includes a transition of this nuclear wave function which can be considered in two limits. One limit is the transition of the ground state from one well into the other [Fig. 20(a)]; w would then be reduced by the overlap of the Gaussian orbitals. The second limit includes virtual transitions into excited oscillator states. This corresponds to a vertical transition [Fig. 20(b)] followed by a relaxation using the anharmonic terms of the oscillator. The direct transition dominates when the two sites are close together, and the vertical transition when the two sites are far apart since the direct transition is exponentially suppressed by the wave-function overlap, while the vertical transition is only suppressed inversely with the intermediate energy (a virtual Franck-Condon transition).[76]

If R_0 and R_2 are the lowest-energy sites of the two oscillators then the Gaussian overlap is

$$\exp[-(M\kappa)^{1/2}(R_2-R_0)^2/4h]\,, \tag{23}$$

which is quite sensitive to the mass of the harmonic oscillator when the two locations are far apart, and not when they are close together. Thus, the isotope shift would be small for sites close together. For sites far apart when the vertical transition dominates, the Gaussian overlap does not enter and the isotope shift is also small. In any case, a large negative-U necessitates relatively large separations between the two sites indicating that vertical transitions are to be expected. This discussion has assumed that the transition rate (given by w) is very small compared to the relaxation rate of the anharmonic oscillator. The actual value of the isotope shift appears to depend on a comparison of the electronic transition rate, with the structural relaxation time of the oscillator which depends

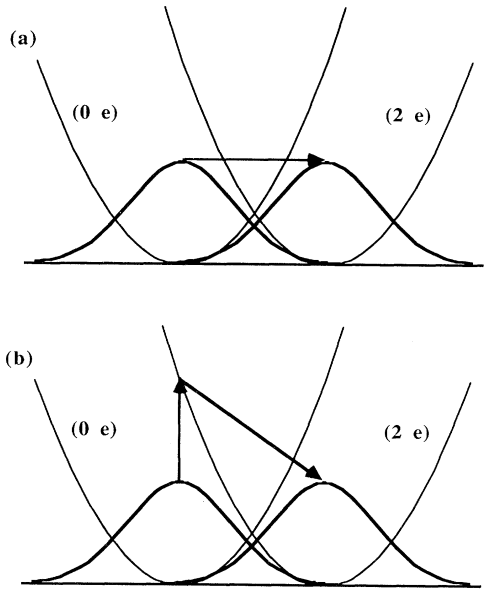

FIG. 20. Illustration of the structural behavior of negative-U centers. The potential experienced by nuclei near the negative-U center (neighboring the oxygen vacancy) is, as usual, approximately parabolic. Two electronic occupations, unoccupied and doubly occupied [Fig. 5(a)], correspond to two different equilibrium positions of the nuclei. The separation between these locations is the relaxation responsible for the negative U. The darker lines are the Gaussian quantum wave functions describing the zero-point motion in the potential wells. The transition between an unoccupied center and a doubly occupied center is illustrated in two limiting cases, (a) direct transition between the two ground states, and (b) a vertical transition followed by a relaxation of the oscillator, assuming an anharmonic oscillator. Because of the transitions between these two states, which are at the same energy, there is a quantum coherence between the two sets of nuclear locations (structural coherence). In the condensed state the coherence is long range because of the long-range order of the condensate.

on the size of anharmonic terms. Experimentally a small and (when detected) very sample-dependent isotope shift has been reported.[77–80] These isotope shift experimental results appear to contradict other experiments, which show a large electron-phonon coupling relevant to superconductivity.[81–83] Within the two-component theory the large electron-phonon coupling is consistent with the small isotope shift.

A signature of the two-component theory, which can take the place of the isotope shift, is "structural coherence." Structural coherence arises because of the quantum superposition of the two separated locations of the nuclei in a negative-U center. The two locations of the negative-U center are basic to the electronic coherence of the superconductivity. Locally, the negative-U center undergoes transitions between the two states in both the uncondensed and condensed states. The quantum state of the center is a linear combination of the occupied and unoccupied states. Thus there is a quantum coherence between the two sets of atomic locations in the uncondensed and condensed states. However, the long-range coherence of the electronic wave function in the condensed state leads to a long-range coherence of the atomic locations as well.

There are three types of experiments which are consistent with this structural coherence. The first type of experiment—infrared[81] and Raman spectroscopies[82,83]—have shown the relevance of electron-phonon coupling to the superconductivity. The second type of experiment is the high-accuracy x-ray- and neutron-diffraction studies which reveal large oval-shaped atomic locations rather than small thermal, more spherical, shapes.[84–86] In 1:2:3:7 material ovals do not appear in the full-plane atoms but are specifically associated with the atoms around the oxygen vacancies—the chain Cu-O and the O above and below the chain. Experimentally it is difficult to know whether these reflect dynamic coherence or static disorder. A direct test of the structural coherence is provided by channeling experiments. In these experiments a beam of ions is directed near to a crystallographic axis. The backscattering of these ions is sensitive to the cross section for encountering an ion. If the nuclear locations become correlated then the cross section should be dramatically affected. Recent experiments[87,88] show that the cross section indeed changes dramatically through the superconducting transition.

Note added. New neutron-diffraction experiments[89] measuring the atomic pair distribution function show direct evidence for the presence of *dynamic local-structural correlations which change at* T_c in a high-T_c Cu-O-based material. New extended x-ray-absorption fine structure (EXAFS) measurements[90] suggest that the oxygen atoms bridging between the chains and the plains in $YBa_2Cu_3O_7$ tunnel between two sites 0.13 Å apart (compare Fig. 20). These results appear to correspond directly to the dynamic structural correlations discussed above.

ACKNOWLEDGMENTS

I wish to thank A. Aharony, M. L. Cohen, D. P. DiVincenzo, T. H. Geballe, Y. Gefen, W. A. Harrison, Y. Imry, M. Kardar, D.-H. Lee, P. A. Lee, S. G. Louie, E. J. Mele, N. D. Mermin, A. J. Millis, V. M. Nabutovskii, L. Pauling, J. C. Phillips, D. J. Scalapino,, H.-B. Schüttler, and D. Vanderbilt for helpful comments and references, and J. M. Vales, Jr. and M. Gurvitch for permission to use the data in Fig. 19. This work was supported in part by the Revson Foundation.

[1]P. Nozières and S. Schmitt-Rink, J. Low Temp. Phys. **59**, 195 (1985).
[2]R. T. Scalettar, E. Y. Loh, J. E. Gubernatis, A. Moreo, S. R. White, D. J. Scalapino, R. L. Sugar, and E. Dagotto, Phys. Rev. Lett. **62**, 1407 (1989).
[3]P. W. Anderson, Phys. Rev. Lett. **34**, 953 (1975).
[4]J. Bardeen, L. N. Cooper, and J. R. Schrieffer, Phys. Rev. **108**, 1175 (1957).
[5]M. Tinkham, *Introduction to Superconductivity* (McGraw-Hill, New York, 1975).
[6]A. Aharony, R. J. Birgeneau, A. Coniglio, M. A. Kastner, and H. E. Stanley, Phys. Rev. Lett. **60**, 1330 (1988).
[7]P. W. Anderson, Science **235**, 1196 (1987).
[8]R. B. Laughlin, Science **242**, 525 (1988).
[9]G. M. Eliashberg, Zh. Eksp. Teor. Fiz. **38**, 966 (1960) [Sov. Phys. JETP **11**, 696 (1960)].
[10]S. Robaszkiewicz, R. Micnas, and K. A. Chao, Phys. Rev. B **23**, 1447 (1981); **24**, 1579 (1981).
[11]J. E. Hirsch and D. J. Scalapino, Phys. Rev. B **32**, 5639 (1985); Phys. Rev. Lett **56**, 2732 (1986).
[12]C. M. Varma, Phys. Rev. Lett. **61**, 2713 (1988).
[13]N. F. Mott, E. A. Davis, and R. A. Street, Philos. Mag. **32**, 961 (1975).
[14]M. Kastner, D. Adler, and H. Fritsche, Phys. Rev. Lett. **37**, 1504 (1976).
[15]G. A. Baraff, E. O. Kane, and M. Schluter, Phys. Rev. B **21**, 5662 (1980).
[16]D. Vanderbilt and J. D. Joannopoulos, Phys. Rev. Lett. **49**, 823 (1982).
[17]R. Car, P. Kelly, A. Oshiyama, and S. T. Pantelides, Phys. Rev. Lett. **52**, 1814 (1984).
[18]Y. Bar-Yam and J. D. Joannopoulos, Phys. Rev. Lett. **56**, 2203 (1986).
[19]G. D. Watkins and J. R. Troxell, Phys. Rev. Lett. **44**, 593 (1980).
[20]J. M. Essick and J. D. Cohen, Phys. Rev. Lett. **64**, 3062 (1990).
[21]A. Fontaine and F. Meunier, Phys. Konden. Mater. **14**, 119 (1972).
[22]C. C. Tsuei and W. L. Johnson, Phys. Rev. B **9**, 4742 (1974).
[23]E. Simánek, Solid State Commun. **32**, 731 (1979).
[24]C. S. Ting, D. N. Talwar, and K. L. Ngai, Phys. Rev. Lett. **45**, 1213 (1980).
[25]H.-B. Schüttler, M. Jarrell, and D. J. Scalapino, Phys. Rev. Lett. **58**, 1147 (1987); Phys. Rev. B **39**, 6501 (1989).
[26]M. R. Schafroth, Phys. Rev. **96**, 1442 (1954).
[27]J. Ranninger and S. Robaszkiewicz, Physica B+C **125B**, 468 (1985).
[28]S. P. Ionov, Izv. Akad. Nauk SSSR Ser. Fiz. **49**, 310 (1985).
[29]G. M. Éliashberg, Pis'ma Zh. Eksp. Teor. Fiz. **46**(S1), 94 (1987) [JETP Lett. **46**, S81 (1987)].

[30]D. M. Newns, Phys. Rev. B **36**, 5595 (1987).
[31]D. M. Newns, M. Rasolt, and P. C. Pattnaik, Phys. Rev. B **38**, 6513 (1988).
[32]J. Ranninger, R. Micnas, and S. Robaszkiewicz, Ann. Phys. (Paris) **13**, 455 (1988).
[33]R. Freidberg and T. D. Lee, Phys. Lett. A **138**, 423 (1989); Phys. Rev. B **40**, 6745 (1989).
[34]L. P. Gorkov and G. M. Éliashberg, Pis'ma Zh. Eksp. Teor. Fiz. **46**(S1), 98 (1987) [JETP Lett. **46**, S84 (1987)].
[35]R. Micnas, J. Ranninger, and S. Robaszkiewicz, Rev. Mod. Phys. **62**, 113 (1990).
[36]H. Suhl, B. T. Matthias, and L. R. Walker, Phys. Rev. Lett. **12**, 552 (1959).
[37]J. Kondo, Prog. Theor. Phys. **29**, 1 (1963).
[38]D. H. Lee and J. Ihm, Solid State Commun. **62**, 811 (1987).
[39]O. Entin-Wohlman and Y. Imry, Physica C **153-155**, 1323 (1988); Phys. Rev. B **40**, 6731 (1989).
[40]J. C. Phillips, Phys. Rev. Lett. **59**, 1856 (1987); Phys. Rev. B **39**, 7356 (1989); and (unpublished).
[41]J. W. Halley and H. B. Shore Phys. Rev. B **37**, 525 (1988).
[42]R. V. Kasowski, W. Y. Hsu, and F. Herman, Phys. Rev. B **36**, 7248 (1987).
[43]W. E. Pickett, Rev. Mod. Phys. **61**, 433 (1989).
[44]R. J. Cava, B. Batlogg, R. B. van Dover, D. W. Murphy, S. Sunshine, T. Siegrist, J. P. Remeika, E. A. Rietman, S. Zahurak, and G. P. Espinosa, Phys. Rev. Lett. **58**, 1676 (1987).
[45]For simplicity the term "mobility" is used throughout to refer to $1/m$; the inverse mass of the carrier. This differs from the mobility of carriers as defined for semiconductors—τ/m where τ is the carrier lifetime. In this paper, the effect of the lifetime is not directly considered in this context. It should be expected that the lifetime will be important if and only if the relevant scattering length is shorter than the superconducting coherence length.
[46]The relative sign between Δ and Δ' is determined by the arbitrary phase of orbitals as defined for $c^\dagger$ and $b^\dagger$ operators.
[47]D. A. Bonn, J. E. Greedan, C. V. Stager, T. Timusk, M. G. Doss, S. L. Herr, K. Kamarás, and D. B. Tanner, Phys. Rev. Lett. **58**, 2249 (1987).
[48]Z. Schlesinger, R. T. Collins, D. L. Kaiser, and F. Holtzberg, Phys. Rev. Lett. **59**, 1958 (1987).
[49]G. A. Thomas, J. Orenstein, D. H. Rapkine, M. Capizzi, A. J. Millis, R. N. Bhatt, L. F. Schneemeyer, and J. V. Waszczak, Phys. Rev. Lett. **61**, 1313 (1988).
[50]R. T. Collins, Z. Schlesinger, F. Holtzberg, and C. Feild, Phys. Rev. Lett. **63**, 422 (1989).
[51]K. Kamarás, S. L. Herr, C. D. Porter, N. Tache, D. B. Tanner, S. Etemad, T. Venkatesen, E. Chase, A. Inam, X. D. Wu, M. S. Hegde, and B. Dutta, Phys. Rev. Lett. **64**, 84 (1990).
[52]M. D. Kirk, D. P. E. Smith, D. B. Mitzi, J. Z. Sun, D. J. Webb, K. Char, M. R. Hahn, M. Naito, B. Oh, M. R. Beasley, T. H. Geballe, R. H. Hammond, A. Kapitulnik, and C. F. Quate, Phys. Rev. B **35**, 8850 (1987).
[53]M. Gurvitch, J. M. Valles, Jr., A. M. Cucolo, R. C. Dynes, J. P. Garno, L. F. Schneemeyer, and J. V. Waszczak, Phys. Rev. Lett. **63**, 1008 (1989).
[54]J. C. Phillips, Phys. Rev. B **41**, 8968 (1990).
[55]P. A. Lee and N. Read, Phys. Rev. Lett. **58**, 2691 (1987).
[56]R. J. Cava, R. B. van Dover, B. Batlogg, and E. A. Rietman, Phys. Rev. Lett. **58**, 408 (1987).
[57]M. K. Wu, J. R. Ashburn, C. J. Torng, P. H. Hor, R. L. Meng, L. Gao, Z. J. Huang, Y. Q. Wang, and C. W. Chu, Phys. Rev. Lett. **58**, 911 (1987).
[58]J. Z. Sun, D. J. Webb, M. Naito, K. Char, M. R. Hahn, J. W. P. Hsu, A. D. Kent, D. B. Mitzi, B. Oh, M. R. Beasley, T. H. Geballe, R. H. Hammond, and A. Kapitulnik, Phys. Rev. Lett. **58**, 1574 (1987).
[59]D. R. Harshman, L. F. Schneemeyer, J. V. Waszczak, G. Aeppli, R. J. Cava, B. Batlogg, L. W. Rupp, E. J. Ansaldo, and D. Ll. Williams, Phys. Rev. B **39**, 851 (1989).
[60]L. Krusin-Elbaum, R. L. Greene, F. Holtzberg, A. P. Malozemoff, and Y. Yeshurun, Phys. Rev. Lett. **62**, 217 (1989).
[61]F. Keffer, in *Ferromagnetism,* Vol. XVIII/2 of *Encyclopedia of Physics,* edited by H. P. J. Wijn and S. Flügge (Springer-Verlag, Berlin, 1966), p. 1.
[62]T. K. Worthington, W. J. Gallagher, and T. R. Dinger, Phys. Rev. Lett. **59**, 1160 (1987).
[63]M. Oda, Y. Hidaka, M. Suzuki, and T. Murakami, Phys. Rev. B **38**, 252 (1988).
[64]U. Welp, W. K. Kwok, G. W. Crabtree, K. G. Vandervoort, and J. Z. Liu, Phys. Rev. Lett. **62**, 1908 (1989).
[65]D. Pines and P. Nozières, *Theory of Quantum Liquids* (Benjamin, New York, 1966).
[66]R. Griessen, Phys. Rev. B **36**, 5284 (1987).
[67]J. T. Makert, J. Beille, J. J. Neumeier, E. A. Early, C. L. Seaman, T. Moran, and M. B. Maple, Phys. Rev. Lett. **64**, 80 (1990).
[68]H. A. Borges, R. Kwok, J. D. Thompson, G. L. Wells, J. L. Smith, Z. Fisk, and D. E. Peterson, Phys. Rev. B **36**, 2404 (1987).
[69]P. Esquinazi, J. Luzuriaga, C. Duran, D. A. Esparza, and C. D'Ovidio, Phys. Rev. B **36**, 2316 (1987).
[70]S. Bhattacharya, M. J. Higgins, D. C. Johnson, A. J. Jacobson, J. P. Stokes, D. P. Goshorn, and J. T. Lewandowski, Phys. Rev. Lett. **60**, 1181 (1988); Phys. Rev. B **37**, 5901 (1988).
[71]D. J. Bishop, A. P. Ramirez, P. L. Gammel, B. Batlogg, E. A. Rietman, R. J. Cava and A. J. Millis, Phys. Rev. B **36**, 2408 (1987).
[72]H. Mathias, W. Moulton, H. K. Ng, S. J. Pan, K. K. Pan, L. H. Peirce, L. R. Testardi and R. J. Kennedy, Phys. Rev. B **36**, 2411 (1987).
[73]P. E. Sulewski, T. W. Noh, J. T. McWhirter, A. J. Sievers, S. E. Russek, R. A. Buhrman, C. S. Jee, J. E. Crow, R. E. Salomon, and G. Myer, Phys. Rev. B **36**, 2357 (1987).
[74]B. Fisher, J. Genossar, I. O. Lelong, A. Kessel, and J. Ashkenazi, J. Supercond. **1**, 53 (1988).
[75]J. Orenstein, G. A. Thomas, A. J. Millis, S. L. Cooper, D. H. Rapkine, T. Timusk, L. F. Schneemeyer, and J. V. Waszczak, Phys. Rev. B **42**, 6342 (1990).
[76]W. A. Harrison, *Solid State Theory* (McGraw-Hill, New York, 1970), p. 333.
[77]B. Batlogg, R. J. Cava, A. Jayaraman, R. B. van Dover, G. A. Kourouklis, S. Sunshine, D. W. Murphy, L. W. Rupp, H. S. Chen, A. White, K. T. Short, A. M. Mujsce, and E. A. Rietman, Phys. Rev. Lett. **58**, 2333 (1987).
[78]L. C. Bourne, M. F. Crommie, A. Zettl, H.-C. zur Loye, S. W. Keller, K. L. Leary, A. M. Stacy, K. J. Chang, and M. L. Cohen, Phys. Rev. Lett. **58**, 2337 (1987).
[79]K. L. Leary, H.-C. Loye, S. W. Keller, T. A. Faltens, W. K. Ham, J. N. Michaels, and A. M. Stacy, Phys. Rev. Lett. **59**, 1236 (1987).
[80]L. C. Bourne, A. Zettl, T. W. Barbee III, and M. L. Cohen, Phys. Rev. B **36**, 3990 (1987).
[81]Y. H. Kim, A. J. Heeger, L. Acedo, G. Stucky and F. Wudl, Phys. Rev. B **36**, 7252 (1987).

[82]D. A. Bonn, J. E. Greedan, C. V. Stager, T. Timiusk, M. G. Doss, S. L. Herr, K. Kamarás and D. B. Tanner Phys. Rev. Lett. **58**, 2249 (1987).
[83]S. L. Cooper, M. V. Klein, B. G. Pazol, J. P. Rice, and D. M. Ginsberg, Phys. Rev. B **37**, 5920 (1988).
[84]M. A. Beno, L. Soderholm, D. W. Capone II, D. G. Hinks, J. D. Jorgensen, J. D. Grace, I. K. Schuller, C. U. Segre, and K. Zhang, Appl. Phys. Lett. **51**, 57 (1987).
[85]A. Williams, G. H. Kwei, R. B. Von Dreele, A. C. Larson, I. D. Raistrick, and D. L. Bish, Phys. Rev. B **37**, 7960 (1988).
[86]J. J. Capone, C. Chaillour, A. W. Hewat, P. Lejay, M. Marezio, N. Nguyen, B. Raveau, J. L. Soubeyroux, J. L. Toulence, and R. Tournier, Europhys. Lett. **3**, 1301 (1987).
[87]R. P. Sharma, L. E. Rehn, P. M. Baldo, and J. Z. Liu, Phys. Rev. Lett. **62**, 2869 (1989).
[88]T. Haga, K. Yamaya, Y. Abe, T. Tajima, and Y. Hidaka, Phys. Rev. B **41**, 826 (1990).
[89]B. H. Toby, T. Egami, J. D. Jorgensen, and M. A. Subramanian, Phys. Rev. Lett. **64**, 2414 (1990).
[90]J. Mustre de Leon, S. D. Conradson, I. Batistić, and A. R. Bishop, Phys. Rev. Lett. **65**, 1675 (1990).